

CONCEPTUAL AERODYNAMIC DESIGN OF RAMJET MISSILES

A THESIS SUBMITTED TO  
THE GRADUATE SCHOOL OF NATURAL AND APPLIED SCIENCES  
OF  
MIDDLE EAST TECHNICAL UNIVERSITY



BY

ERTAN DEMİRAL

IN PARTIAL FULFILLMENT OF THE REQUIREMENTS  
FOR  
THE DEGREE OF MASTER OF SCIENCE  
IN  
AEROSPACE ENGINEERING

JANUARY 2017



Approval of the thesis

**CONCEPTUAL AERODYNAMIC DESIGN OF RAMJET MISSILES**

submitted by **ERTAN DEMİRAL** in partial fulfillment of the requirements for the degree of **Master of Science in Aerospace Engineering Department, Middle East Technical University** by,

Prof. Dr. Gülbin Dural Ünver  
Dean, Graduate School of **Natural and Applied Sciences**

\_\_\_\_\_

Prof. Dr. Ozan Tekinalp  
Head of Department, **Aerospace Engineering**

\_\_\_\_\_

Assoc. Prof. Dr. Sinan Eyi  
Supervisor, **Aerospace Engineering Dept., METU**

\_\_\_\_\_

**Examining Committee Members:**

Prof. Dr. İsmail Hakkı Tuncer  
Aerospace Engineering Dept., METU

\_\_\_\_\_

Assoc. Prof. Dr. Sinan Eyi  
Aerospace Engineering Dept., METU

\_\_\_\_\_

Prof. Dr. Hüseyin Nafiz Alemdaroğlu  
Department of Airframe and Powerplant Maintenance.,  
Atılım Uni.

\_\_\_\_\_

Prof. Dr. Serkan Özgen  
Aerospace Engineering Dept., METU

\_\_\_\_\_

Asst. Prof. Dr. Durmuş Sinan Körpe  
Aeronautical Engineering Dept.,  
University of Turkish Aeronautical Association

\_\_\_\_\_

**Date: 25/01/2017**



**I hereby declare that all the information in this document has been obtained and presented in accordance with academic rules and ethical conduct. I also declare that, as required by these rules and conduct, I have fully cited and referenced all material and results that are not original to this work.**

Name, Last name : Ertan Demiral

Signature :

## **ABSTRACT**

### **CONCEPTUAL AERODYNAMIC DESIGN OF RAMJET MISSILES**

Demiral, Ertan  
M.S., Department of Aerospace Engineering  
Supervisor: Assoc. Prof. Dr. Sinan Eyi

January 2017, 87 Pages

The prediction of aerodynamic coefficients of missiles that have air-breathing components is a challenging task during the preliminary design phase. It is considerably important to estimate missile aerodynamic coefficients accurately at the beginning of design phase to avoid poor designs which could lead to redesign at later stages of the design process. In this study, firstly an improved method is developed to predict the aerodynamic coefficients of missile configurations with air-breathing components more accurately compared to engineering level fast prediction tools. Then, optimization studies comprising of reaching global minimum value of the Beale Function and inverse design optimization of the ramjet missile configuration are done through implementing different meta-heuristic optimization techniques which are “Genetic Algorithm”, “Differential Evolution” and “Modified Cuckoo Search”. In the inverse design optimization studies, two different methods, which are engineering level fast prediction tool Missile DATCOM and the improved method, are used to calculate aerodynamic coefficients of the candidate missile

configurations throughout the design optimization process. Results of the inverse design optimization studies show that preliminary design phase of the missiles including air-breathing components can be enhanced significantly since accuracy of the prediction of aerodynamic coefficients is improved by methods applied in this study.

Keywords: Ramjet Missiles, Metaheuristic Optimization Algorithms, Computational Fluid Dynamics, Fast Prediction Tools, Component Build Up Method



## ÖZ

### RAMJET FÜZELERİN KAVRAMSAL AERODİNAMİK TASARIMI

Demiral, Ertan

Yüksek Lisans, Havacılık ve Uzay Mühendisliği Bölümü

Tez Yöneticisi: Assoc. Prof. Dr. Sinan Eyi

Ocak 2017, 87 Sayfa

Hava solunmalı bileşenlere sahip füzelerin aerodinamik katsayılarının tahmini öntasarım aşamasında oldukça zordur. Tasarım aşaması başlangıcında aerodinamik katsayıların doğru bir şekilde tahmin edilmesi, tasarım sürecinin ileriki aşamalarında yeniden tasarıma sebep olabilecek kötü tasarımlardan kaçınılması için oldukça önemlidir. Bu çalışmada ilk olarak, hava solunmalı füze konfigürasyonlarının aerodinamik katsayılarını mühendislik seviyesi hızlı tahmin araçlarına göre daha doğru tahmin edebilecek ileri bir yöntem geliştirilmiştir. Daha sonra ise, üstsezgisel optimizasyon tekniklerinden (“Genetic Algorithm”, “Differential Evolution” ve “Modified Cuckoo Search”) faydalanılarak Beale fonksiyonunun global en küçük değerine ulaşma ve ramjetli füze konfigürasyonunun tersine tasarım optimizasyonu çalışmaları gerçekleştirilmiştir. Tersine tasarım optimizasyonu çalışmalarında, tasarım optimizasyonu sürecinde oluşturulan füze konfigürasyonlarının aerodinamik katsayılarını hesaplamak için, mühendislik seviyesi hızlı tahmin aracı Missile DATCOM ve geliştirilmiş yöntem olmak üzere, iki farklı metottan faydalanılmıştır.

Tersine tasarım optimizasyonu alıřmaları sonularının gsterdiĐi zere, bu alıřmada uygulanan metotlar ile aerodinamik katsayıların tahmin doĐrulukları arttırıldıĐı iin hava solumalı bileřenlere sahip fzelerin n tasarım sreci nemli derecede iyileřtirilebilir.

Anahtar Kelimeler: Ramjet Fzeleri, stsezgisel Optimizasyon Algoritmaları, Hesaplmalı Akıřkanlar DinamiĐi, Hızlı Tahmin Araları, Bileřen İnřa Yntemi





*To My Family*

## ACKNOWLEDGEMENTS

I would first like to thank my supervisor Assoc. Prof. Dr. Sinan EYİ for continuous support, advice and criticism throughout the thesis study.

I would like to thank my colleagues in Aerodynamics Division of ROKETSAN for their help and motivation during the thesis.

I would like to thank Mr. Kİvanç ARSLAN, Mr. Batuhan NASUHBEOĞLU and Mr. Engin USTA for their valuable friendship and support during this study.

Finally, I must express my very profound gratitude to my wife Mrs. Merve DEMİRAL, and my parents Mr. Habil DEMİRAL, Mrs. Fatma DEMİRAL for providing their help and motivation. This accomplishment would not have been possible without them.

## TABLE OF CONTENTS

<b>ABSTRACT .....</b>	<b>V</b>
<b>ÖZ.....</b>	<b>VII</b>
<b>ACKNOWLEDGEMENTS.....</b>	<b>X</b>
<b>TABLE OF CONTENTS.....</b>	<b>XI</b>
<b>LIST OF TABLES .....</b>	<b>XIII</b>
<b>LIST OF FIGURES .....</b>	<b>XIV</b>
<b>CHAPTERS</b>	
<b>INTRODUCTION.....</b>	<b>1</b>
1.1 Concept of Ramjet Engine .....	2
1.2 Fast Prediction Tools .....	7
1.3 Meta-heuristic Optimization Algorithms .....	8
1.4 Aerodynamic Coefficients and Coordinate System .....	8
1.5 Literature Survey.....	9
1.6 Aim of Thesis .....	14
<b>VALIDATION.....</b>	<b>17</b>
2.1 Validation 1: Validation of Aerodynamic Analyses Tools .....	17
2.2 Validation 2: Validation of Meta-Heuristic Optimization Algorithms .....	25
<b>METHODOLOGY.....</b>	<b>31</b>
3.1 The Fast Prediction Method (Missile DATCOM) .....	31
3.2 Improvements on Fast Prediction Method (Improved Method) .....	32
3.3 CAD, Grid Generator, CFD and Post Processing Tools .....	48
3.4 Optimization Algorithms .....	51
3.4.1 Cuckoo Search Algorithm.....	51
3.4.2 Modified-Cuckoo Search Algorithm .....	52
3.4.3 Differential Evolution .....	55
3.4.4 Genetic Algorithm.....	57
<b>RESULTS AND DISCUSSION .....</b>	<b>59</b>

4.1 Design Variables and Objective Function.....	60
4.2 Case 1: Inverse Design Optimization Studies with Fast Prediction Method (Missile DATCOM) .....	62
4.3 Case 2: Inverse Design Optimization Studies with Improved Method .....	68
<b>CONCLUSION.....</b>	<b>81</b>
<b>REFERENCES.....</b>	<b>83</b>



## LIST OF TABLES

Table 1: Model Data Comparison [9] .....	10
Table 2: Data Comparison [11].....	11
Table 3: Explanation of numbers in Figure 15.....	14
Table 4: Comparison of optimization algorithms (Iteration Number) with Beale Function .....	27
Table 5: Comparison of optimization algorithms (Function Evaluation Number) with Beale Function .....	28
Table 6: Explanation of the subscripts .....	32
Table 7: Explanation of the subscripts .....	34
Table 8: Lower and upper limits of design variables.....	61
Table 9: Summary of converged iteration numbers of optimization algorithms .....	63
Table 10: Assigned values of the optimization algorithm parameters.....	69
Table 11: Comparison of the optimum configurations obtained at the end of the design optimization studies .....	78

## LIST OF FIGURES

Figure 1: Representative and descriptive figure of a ramjet engine [2] .....	2
Figure 2: Specific impulse as a function of the flight Mach number for selected engine cycles [3].....	3
Figure 3: Classification of ramjets with inlet types [3].....	4
Figure 4: Weighted Selection Factors for Different Inlet Types [3] .....	5
Figure 5: Advanced Strategic Air Launched Missile (1965-80) [5] .....	6
Figure 6: GQM-163A Coyote (2002-Today) [5] .....	6
Figure 7: Meteor (2016-Today) [6].....	6
Figure 8: P-270 Moskit (1984-Today) [7].....	6
Figure 9: Talos (1950-Today) [8].....	7
Figure 10: Demonstration of aerodynamic coefficients on a representative missile configuration .....	9
Figure 11: Geometry Comparison [9] .....	10
Figure 12: SASM [11].....	11
Figure 13: Pareto Front designs obtained from multi-objective optimization [12]....	11
Figure 14: No-Escape Zone (NEZ) comparison for conventional and ramjet missile [13] .....	12
Figure 15: Comparison of Genetic Algorithm (GA), Particle Swarm Optimization (PSO) and Cuckoo Search (CS) [21].....	13
Figure 16: Ramjet missile configuration.....	18
Figure 17: Axial force coefficient validation comparison (Mach=2.5, Re=6.56E+6)	18
Figure 18: Normal force coefficient validation comparison (Mach=2.5, Re=6.56E+6) .....	19
Figure 19: Pitching moment force coefficient validation comparison (Mach=2.5, Re=6.56E+6) .....	19
Figure 20: Axial force coefficient validation comparison (Mach=2.95, Re=6.56E+6) .....	20

Figure 21: Normal force coefficient validation comparison (Mach=2.95, Re=6.56E+6).....	20
Figure 22: Pitching moment force coefficient validation comparison (Mach=2.95, Re=6.56E+6).....	21
Figure 23: Axial force coefficient validation comparison (Mach=3.5, Re=6.56E+6)	21
Figure 24: Normal force coefficient validation comparison (Mach=3.5, Re=6.56E+6).....	22
Figure 25: Pitching moment force coefficient validation comparison (Mach=3.5, Re=6.56E+6).....	22
Figure 26: Close view of the computational volume grid.....	23
Figure 27: Static Pressure distribution over missile surface and Mach Contour over XY plane (Mach=2.5, Re=6.56E+6, $\alpha=15^\circ$ ).....	23
Figure 28: Static Pressure distribution over missile body surface (Mach=2.5, Re=6.56E+6, $\alpha=15^\circ$ ).....	24
Figure 29: Static Pressure distribution over missile body surface and Total Pressure distribution over cut planes (Mach=2.5, Re=6.56E+6, $\alpha=15^\circ$ ).....	24
Figure 30: Beale's function plot [23].....	25
Figure 31 Comparison of fitness values of optimization algorithms (IRN=15685) ..	26
Figure 32 Comparison of fitness values of optimization algorithms (IRN=37329) ..	26
Figure 33: Comparison of fitness values of optimization algorithms (IRN=81653) .	27
Figure 34: Comparison of optimization algorithms including referenced MCS algorithm with Rosenbrock function (d=10).....	28
Figure 35: Ramjet missile configuration.....	33
Figure 36: Combined body (Body +Ramjet) .....	33
Figure 37: Tail Fin Set .....	33
Figure 38: Combined body axial force coefficient validation comparison (Re=6.56E+6)	35
Figure 39: Combined body normal force coefficient validation comparison (Re=6.56E+6).....	35
Figure 40: Combined body pitching moment coefficient validation comparison (Re=6.56E+6).....	36

Figure 41: Tail fin axial force coefficient validation comparison (Re=6.56E+6).....	37
Figure 42: Tail fin normal force coefficient validation comparison (Re=6.56E+6) ..	37
Figure 43: Tail fin pitching moment coefficient validation comparison (Re=6.56E+6) .....	38
Figure 44: Comparison of computed tail in the presence of body interference factors .....	39
Figure 45: Comparison of computed body in the presence of tail interference factors .....	39
Figure 46: Variation of tail in the presence body interference factors with respect to different missile body diameters (M=2.5).....	40
Figure 47: Variation of body in the presence tail interference factors with respect to different body diameters (M=2.5).....	41
Figure 48: Variation of tail in the presence body interference factors with respect to different span values (M=2.5).....	42
Figure 49: Variation of body in the presence tail interference factors with respect to different span values (M=2.5).....	42
Figure 50: Variation of tail in the presence body interference factors with respect to different leading edge positions (M=2.5).....	43
Figure 51: Variation of body in the presence tail interference factors with respect to different leading edge positions (M=2.5).....	44
Figure 52: Percentage error analyses of $C_N$ calculated with MD and Fluent Interference Factors (M=2.5).....	45
Figure 53: Percentage error analyses of $C_{m  _{x_{cg}}}$ calculated with MD and Fluent Interference Factors (M=2.5).....	45
Figure 54: Percentage error analyses of $C_N$ calculated with MD and Fluent Interference Factors (M=2.95).....	46
Figure 55: Percentage error analyses of $C_{m  _{x_{cg}}}$ calculated with MD and Fluent Interference Factors (M=2.95).....	46
Figure 56: Percentage error analyses of $C_N$ calculated with MD and Fluent Interference Factors (M=3.5).....	47

Figure 57: Percentage error analyses of $C_m  _{x_{cg}}$ calculated with MD and Fluent Interference Factors ( $M=3.5$ ) .....	47
Figure 58: Comparison of turbulence models [26] .....	49
Figure 59: Generation of trial vector for two-dimensional space .....	55
Figure 60: Crossover operation .....	58
Figure 61: Mutation operation .....	58
Figure 62: Representation of design variables on missile configuration .....	60
Figure 63: Change of fitness value ( $F_{Total}$ ) with respect to iteration number (IRN=12017).....	63
Figure 64: Change of fitness value ( $F_{Total}$ ) with respect to iteration number (IRN=35871).....	64
Figure 65: Change of fitness value ( $F_{Total}$ ) with respect to iteration number (IRN=77865).....	64
Figure 66: Configuration history of the design optimization studies (IRN=12017)..	65
Figure 67: Configuration history of the design optimization studies (IRN=35871)..	66
Figure 68: Configuration history of the design optimization studies (IRN=77865)..	67
Figure 69: Fitness value variation of the design optimization studies .....	69
Figure 70: Comparison of the sub-objective functions in 3D .....	70
Figure 71: Demonstration of improved method output data with pareto designs.....	71
Figure 72: Demonstration of improved method output data with pareto designs.....	71
Figure 73: Demonstration of improved method output data with pareto designs.....	72
Figure 74: Parallel coordinates plots of improved method pareto designs .....	72
Figure 75: Presentation of improved method pareto design configurations for total objective function and each sub-objective function.....	73
Figure 76: Comparison of the sub-objective functions in 3D .....	74
Figure 77: Demonstration of Missile DATCOM output data with pareto designs ....	74
Figure 78: Demonstration of Missile DATCOM output data with pareto designs ....	75
Figure 79: Demonstration of Missile DATCOM output data with pareto designs ....	75
Figure 80: Parallel coordinates plots of Missile DATCOM pareto designs .....	76
Figure 81: Presentation of Missile DATCOM pareto design configurations for total objective function and each sub-objective function.....	77



## CHAPTER 1

### INTRODUCTION

Ramjet engines which have significantly increased propulsion performance of the systems have been started to be used for missiles since 1930s [1]. A missile with air breathing components and flying efficiently at high supersonic speed regimes where Mach number is nearly between two and five may be called as “ramjet missile”. These kinds of missiles become more of an issue when the speed of missile gains importance. They are preferred to conventional missiles due to their high specific impulse values at high speeds. In literature, there are many types of ramjet missiles designed and manufactured for various missions. Classification of these missiles is made depending upon different key aspects such as launching mode, inlet type, range etc.

In preliminary design stage of missiles, aerodynamic coefficients, which are used to measure aerodynamic performance competence of configurations, are generally obtained by using fast prediction analyses tools. The common problem experienced with these tools is that aerodynamic coefficients are usually predicted inaccurately for ramjet missile configurations. Inaccurate estimation of these coefficients are mainly stem from wrong prediction of interference effects between missile components due to unconventional shape and incapability of modeling the internal flows existing on missile aerodynamics. Therefore, first objective of this study is to develop an alternative method to fast prediction tools, which can be used to calculate aerodynamic coefficients of ramjet missile configurations more accurately. Second objective of this research is to perform inverse design optimization studies considering the target ramjet missile configuration shown in Figure 16. Inverse

design activities are done employing different meta-heuristic optimization algorithms and best optimization algorithm is determined by analyzing the results of inverse design studies.

To conclude, it is desired to show in this study that design optimization tasks conducted with developed method and selected optimization algorithm will quickly reveal optimum missile configurations which surely satisfy specified aerodynamic performance requirements.

### 1.1 Concept of Ramjet Engine

In high speed flights, ramjet engines are preferred thanks to their low weight, high specific impulse and simpler designs. Apart from other types of engines such as turbojet, turbofan etc., ramjet engines do not have any moving machinery parts. Representative and descriptive figure of a ramjet engine can be seen in Figure 1:

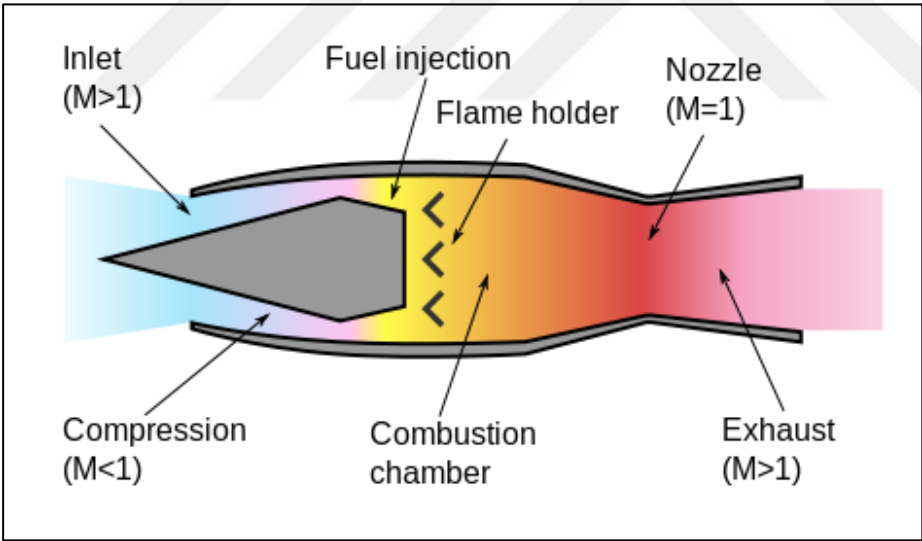


Figure 1: Representative and descriptive figure of a ramjet engine [2]

As shown in Figure 1, ramjet engines consist of inlet, combustor and nozzle sections. Generation of thrust using a ramjet engine can be summarized in three steps as follows:

1. Air is compressed in inlet section and brought into combustor part with high static pressure (converted from dynamic pressure)
2. Combustion takes place by adding some amount fuel to compressed air and then igniting.
3. Hot exhaust gases arising as a result of combustion process accelerate through nozzle part and produce thrust.

For a ramjet engine, there is no need of any moving machinery part to compress air since it is succeeded by generated shock waves at the inlet. Despite these shock waves provide the combustion process to be taken place in subsonic speeds, they substantially contribute to performance losses. Loss rate increases as vehicle Mach number increases. Therefore, at hypersonic speeds where Mach number is greater than five, ramjet propulsion systems become inefficient. Performance comparison of the engines having different types of propulsion systems can be seen in Figure 2:

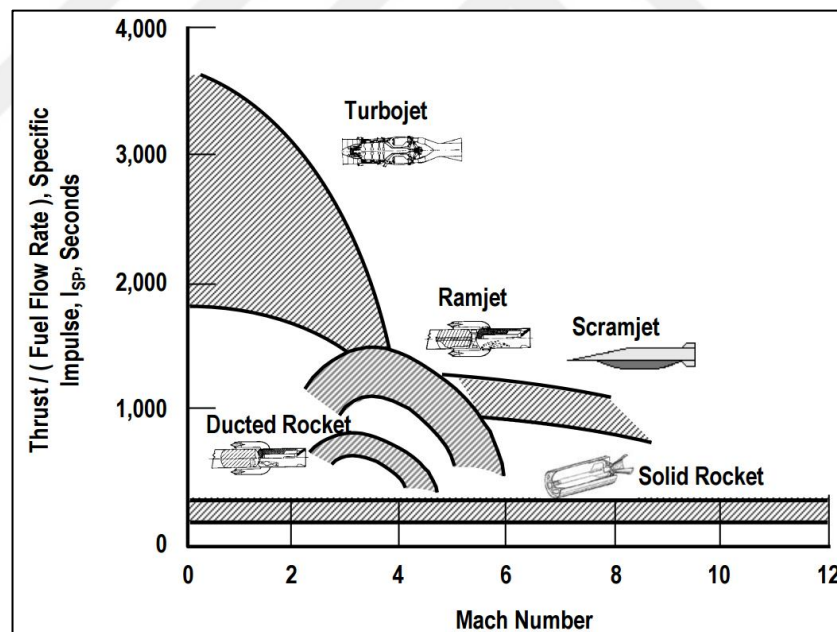


Figure 2: Specific impulse as a function of the flight Mach number for selected engine cycles [3]

In the design process of ramjet missile, main design considerations taken into account for the ramjet component are opening type, inlet placement and number of

inlets. Different types of ramjet inlets mounted on a particular missile body are presented in Figure 3:



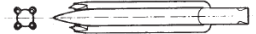
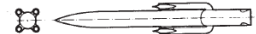
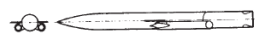




Type Inlet	Sketch	Placement
Nose		Nose-full axisymmetric
Chin		Forward underside in nose compression field-partial axisymmetric
Forward Cruciform Axisymmetric		Forward in nose compression field-cruciform ( four ) axisymmetric
Aft Cruciform Axisymmetric		Aft-cruciform ( four ) axisymmetric
Underwing Axisymmetric		In planar wing compression field-twin axisymmetric
Twin Two-dimensional		Aft-twin cheek-mounted two-dimensional
Underslung Axisymmetric		Aft underside-full axisymmetric
Underslung Two-dimensional		Aft underside-belly mounted two-dimensional
CruciformTwo-dimensional		Aft-cruciform ( four ) two-dimensional

Figure 3: Classification of ramjets with inlet types [3]

During the design process of ramjet component, the best trade-off study between possible inlet types can be successfully completed based on the selection factors presented in Figure 4. For a ramjet missile, it is desired to have:

- Higher pressure recovery
- Small carriage envelope on the launch platform
- High angle of attack capability
- Light weight
- Low cost
- No shrouding of the warhead
- Preferred steering approach (skid to turn, bank to turn)
- Preferred type of flight control (tail, canard, wing)
- Preferred mission application (air to surface (ATS), air to air (ATA), surface to air (STA))

Type Inlet	Selection Factors										
	Pressure Recovery	Carriage Envelope	Alpha Capability	Weight	Drag	Warhead Shrouding	inlet Cost	Preferred Steering	Preferred Control	Prime Mission Suitability	
	●	●	○	●	●	-	●	STT	W, C	ATS, STA	
	●	●	●	○	●	○	○	BTT	T	ATS, ATA, STA	
	●	○	●	-	○	-	-	STT	T	ATS, ATA, STA	
	○	●	○	●	○	●	○	STT	T	ATS	
	●	-	●	●	○	●	●	BTT	T	ATA, STA	
	●	○	●	●	●	●	○	BTT	T	ATS, ATA, STA	
	○	-	○	●	○	●	●	BTT	T	ATS	
	-	-	●	●	●	●	●	BTT	T	ATS, ATA, STA	
	-	○	○	●	●	●	○	STT	T	ATS	

Note:  
 BTT = Bank to Turn  
 STT = Skid to Turn  
 W = Wing C = Canard  
 T = Tail

● Superior   ● Above Average   ○ Average   - Below average

Figure 4: Weighted Selection Factors for Different Inlet Types [3]

It is not possible for a missile inlet to be the best in all of the stated selection factors. Therefore, inlet type selection is achieved with weighted selection factors to determine optimum inlet configuration.

In this study, inlet type selection is not investigated. Throughout the study, ramjet missile used for optimization analysis has twin two-dimensional inlet [4]. Comparison of this inlet type with others with respect to selection factors can be seen in Figure 4.

Some of the example ramjet missiles with different inlet types can be seen in Figure 5-9:

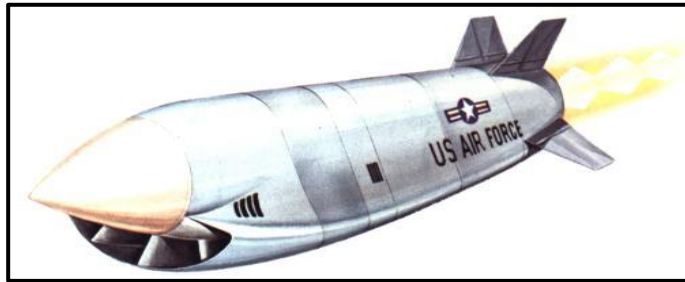


Figure 5: Advanced Strategic Air Launched Missile (1965-80) [5]



Figure 6: GQM-163A Coyote (2002-Today) [5]



Figure 7: Meteor (2016-Today) [6]



Figure 8: P-270 Moskit (1984-Today) [7]



Figure 9: Talos (1950-Today) [8]

## 1.2 Fast Prediction Tools

In the missile configuration design processes, aerodynamic analyses of configurations are mostly succeeded by employing engineering level fast prediction tools and computational fluid aerodynamic (CFD) tools. These tools are different from each other in terms of accuracy and computational cost. While CFD tools have high accuracy and high computational cost, fast prediction tools have low accuracy and low computational cost. During the preliminary design phase, aerodynamic analyses should be achieved quickly since many alternative design configurations are evaluated concurrently. In this phase, fast prediction tools, which are usually necessary due to time and computational cost constraints, are preferable since it is important to predict aerodynamic coefficients of missile configurations in a rapid manner.

After an extensive review of the literature, some of the commonly used fast prediction tools can be listed as follows:

- Missile DATCOM (MD09)
- AeroPrediction (AP)
- MISL3
- MISDL

All of the above tools may be preferred for time and computational cost constraints. However, only Missile DATCOM is capable of partially modeling and analyzing the ramjet component of missile configurations. For this reason, Missile DATCOM is used throughout this study since the model to be analyzed has ramjet components.

### **1.3 Meta-heuristic Optimization Algorithms**

Optimization studies have been carried out for many years in numerous fields such as engineering design, computer-aided molecular design, finance and investment strategies etc. These studies have been achieved thanks to developed optimization algorithms which can be categorized as gradient-free and gradient-based algorithms. This categorization depends on whether derivative information about the problem, which is obtained during solution stage, exists or not. For gradient-based algorithms, type of the problem should be suitable for getting derivative information. In these algorithms, the optimum solution can be found quickly but with a high risk of getting the local optimum solution in the solution domain where there usually might exist local optimum solutions in addition to global optimum solution. For gradient free algorithms, gradient information is not used at solution stage. With these algorithms, it is highly possible to get global optimum solution in the solution domain.

Gradient-free algorithms can also be categorized as deterministic and meta-heuristic. Deterministic techniques do not include randomness whereas meta-heuristic algorithms utilize initial random numbers to drive optimization. Even though deterministic techniques usually converge to local optimum, it is commonly used in industry due to its simplicity. In this work, it is mainly focused on metaheuristic optimization algorithms to get global optimum point in the solution domain.

### **1.4 Aerodynamic Coefficients and Coordinate System**

In this paper, all the predicted aerodynamic coefficients are given with respect to body-fixed coordinate system. Demonstration of aerodynamic coefficients (two forces and one moment) on a representative missile configuration with respect to body-fixed coordinate system can be seen in Figure 10:

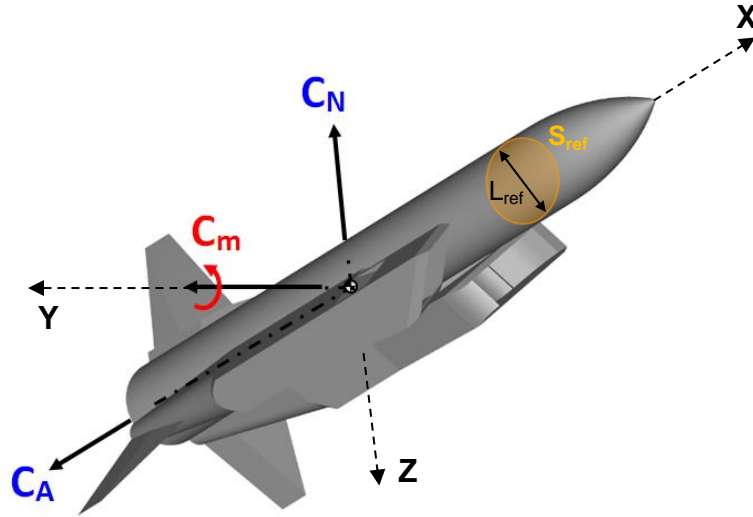


Figure 10: Demonstration of aerodynamic coefficients on a representative missile configuration

Forces and moments can be converted to non-dimensional forms by appropriate terms. In this study, an attempt to predict Axial Force (A), Normal Force (N) and Pitching Moment (m) is made. The predicted moment and forces are nondimensionalized with appropriate terms as follows:

$$C_A = \frac{\text{Axial Force}}{1/2 \rho_{\infty} V^2 S_{ref}}, \quad C_N = \frac{\text{Normal Force}}{1/2 \rho_{\infty} V^2 S_{ref}}, \quad C_m = \frac{\text{Pitching Moment}}{1/2 \rho_{\infty} V^2 S_{ref} L_{ref}}$$

Reference length ( $L_{ref}$ ) and reference area ( $S_{ref}$ ) parameters correspond to the missile body diameter and cross-section area of the missile body at yz plane.

## 1.5 Literature Survey

In literature, studies related to optimization of the ramjet powered missiles usually involve the optimization of missile aerodynamic shape and aeropropulsive systems. For missile aerodynamic shape optimization, missile diameter, missile length, missile nose geometry and its length, number of fins, fin shape and fin dimensions (chord, span, taper ratio) are critical parameters to be determined. On the other hand, for aeropropulsive system optimization, fuel consumption rate, mass flow rate, total pressure recovery, inlet shape and its dimensions, nozzle shape and its dimensions are crucial. It is required to determine all of these stated parameters in order to

achieve ramjet powered missile design optimization. In this part, details of the studies in literature related to optimization of missile aerodynamic shape and aeropropulsive systems are given.

A preliminary design study about design optimization of symmetric-centerbody ramjet powered missile using genetic algorithm is performed by Hartfield, Jenkins and Burkhalter [9]. Design optimization study, which is carried out with driven genetic algorithm method and supporting suite of codes, consists of the missile aerodynamic shape design as well as the detailed preliminary design of inlet, warhead, combustor and nozzle section. Validation works are also accomplished for the implemented method with inversely design of existing ramjet missile Kh-31. Even though the model configuration used in validation work has fundamental differences than Kh-31 missile, results show that implemented method is reliable for ramjet missile modelling.

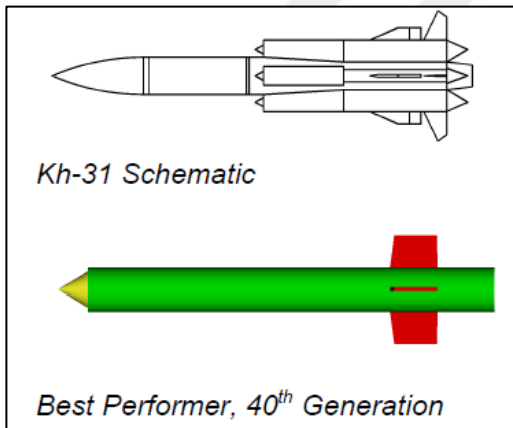


Table 1: Model Data Comparison [9]

	Kh-31	Modeled Missile
Diameter	1.2	1.44
Length	15.4	14.37
Total Weight	1320	1241.5

Figure 11: Geometry Comparison [9]

Study of the Anderson, Burkhalter and Jenkins [10] indicate that genetic algorithm is a powerful tool that can be used to determine highly efficient and robust missile aerodynamic designs for both single and multiple goal applications.

Baratech, Ceva, Chaklos, Martinez, Winkelmann and Ravindra [11] proposed a study for preliminary design of a ramjet powered Supersonic Anti-Ship Missile (SASM). Design study involves the aerodynamics sizing analyses, propulsion system analyses,

structural analyses, stability analyses as well as testing of the configuration in the supersonic tunnels at Parks College of Saint Louis University. In the study, test drag coefficients and calculated drag coefficients of DATCOM method are compared, and results show that test drag values are about 20% lower than the calculated drag values.

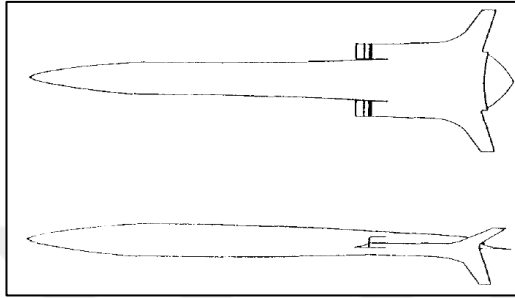


Figure 12: SASM [11]

Table 2: Data Comparison [11]

	$C_{d0}(\alpha=0^\circ)$	$C_d(\alpha=1.25^\circ)$
Test	0.128	0.137
Calculated	0.137	0.172
%Diff.	24%	20%

In the study of Gaiddon and Knight [12], mono-objective and multi-objective missile design optimization considering the missile global performance parameters (range, maneuverability and cruise) is achieved changing the inlet geometric parameters and capture area. Results of the study clearly show that Pareto Front is a powerful method which can be used in order to find the best trade-off between several parameters.

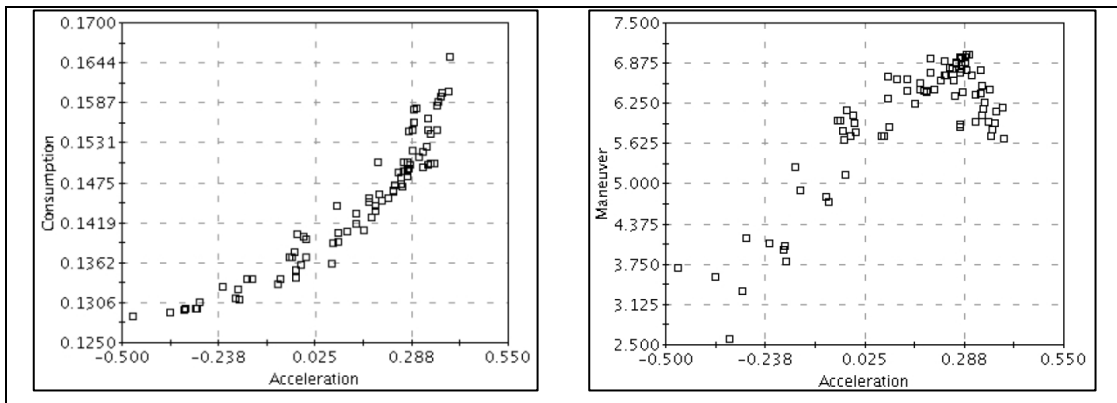


Figure 13: Pareto Front designs obtained from multi-objective optimization [12]

Performance comparison of the missile having ramjet propulsion and conventional rocket motor propulsion is carried out as a result of the collaborative work of the TNO Prins Maurits Laboratory and Canadian Defence Research Establishment Valcartier (DREV) [13]. Results of the study show that No-Escape Zone (NEZ) of the ramjet propulsion systems is 2-2.5 times greater than conventional propulsion systems.

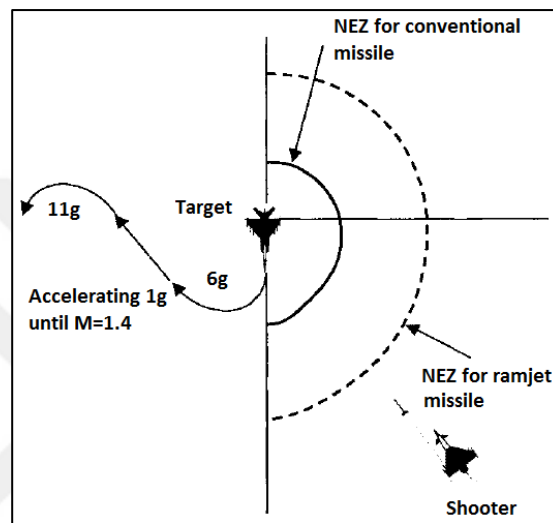


Figure 14: No-Escape Zone (NEZ) comparison for conventional and ramjet missile [13]

The study of Herling, Saheli, Holcomb and Hanson [14] involves the prediction of the steady three-dimensional aerodynamics of a supersonic ramjet missile by employing three different CFD methods which are Parabolized Navier-Stokes (PNS), Euler and Linearized Potential Flow.

Analytic relationships between supersonic missile aerodynamic characteristics (lift, zero-lift drag and drag due-to-lift) and performance parameters (range, velocity, flight path angle and maneuver load factor) are developed in the study of Krieger [15] for preliminary performance estimates and to identify desirable aerodynamic, propulsion and design features.

Reverse engineering of solid rocket missiles is investigated in the study of Metts, Hartfield, Burkhalter and Jenkins [16]. In this study, the purpose is to find design

configurations that closely match the performance characteristics of the baseline model by employing Genetic Algorithm. Arslan [17] has also performed inverse design activities for conventional missile configurations utilizing both gradient-free and gradient based algorithms and showed that gradient-based algorithm has difficulties on locating global optimum point in a complex search space.

Design optimization of liquid propellant missile systems is accomplished by implementing genetic algorithm for multiple goals and configurations through the study of Riddle, Hartfield, Burkhalter and Jenkin [18]. During the optimization stage, aerodynamic database of the missile configurations is obtained by means of the fast predictors of Missile DATCOM and Aerodsn due to their low computational costs.

Carpenter, Hartfield and Burkhalter [19] has also developed an alternative method, which is multivariable function approximation approach using statistical learning techniques such as projection pursuit regression, neural networks and multivariate nonlinear regression, to existing fast prediction tools to enable the reliable prediction of integrated aerodynamic characteristics of missiles. Çetiner [20] has also developed an enhanced semi-empirical engineering-level method enabling more accurate prediction of missile aerodynamic coefficients.

Functions/Algorithms	GA	PSO	CS
Multiple peaks	52124 ± 3277(98%)	3719 ± 205(97%)	927 ± 105(100%)
Michalewicz's ( $d=16$ )	89325 ± 7914(95%)	6922 ± 537(98%)	3221 ± 519(100%)
Rosenbrock's ( $d=16$ )	55723 ± 8901(90%)	32756 ± 5325(98%)	5923 ± 1937(100%)
De Jong's ( $d=256$ )	25412 ± 1237(100%)	17040 ± 1123(100%)	4971 ± 754(100%)
Schwefel's ( $d=128$ )	227329 ± 7572(95%)	14522 ± 1275(97%)	8829 ± 625(100%)
Ackley's ( $d=128$ )	32720 ± 3327(90%)	23407 ± 4325(92%)	4936 ± 903(100%)
Rastrigin's	110523 ± 5199(77%)	79491 ± 3715(90%)	10354 ± 3755(100%)
Easom's	19239 ± 3307(92%)	17273 ± 2929(90%)	6751 ± 1902(100%)
Griewank's	70925 ± 7652(90%)	55970 ± 4223(92%)	10912 ± 4050(100%)
Shubert's (18 minima)	54077 ± 4997(89%)	23992 ± 3755(92%)	9770 ± 3592(100%)

Figure 15: Comparison of Genetic Algorithm (GA), Particle Swarm Optimization (PSO) and Cuckoo Search (CS) [21]

Yang and Deb [21] proposed a new metaheuristic algorithm of cuckoo search which is inspired from brood parasitic behavior of some birds and fruit flies. The validation and comparison of this algorithm with other algorithms such as genetic algorithm

and particle swarm algorithm has been carried out and results show that cuckoo search is much more efficient in finding the global optima with higher success rates.

Table 3: Explanation of numbers in Figure 15

<b>927 ± 105(100%)</b>		
<b>927</b>	:	Average number (mean) of function evaluations
<b>105</b>	:	Standard deviation
<b>100%</b>	:	The success rate of finding the global optima

Walton [22] has shown in his study that gradient free optimization algorithms can be used for engineering applications. In his study, he developed improved cuckoo search algorithms by modifying the levy flight coefficient and crossover method of the original cuckoo search algorithm for better convergence speed, and then implemented this improved method for aerodynamic shape optimization for airfoil improvement and reduced order mesh optimization.

## 1.6 Aim of Thesis

Aerodynamic configuration design of missiles having air-breathing inlet components by employing fast prediction tools is challenging. Since more detailed analyses are necessary due to addition of air-breathing component to missile configuration, results of these tools are usually not within the accuracy constraints. In this study, it is firstly aimed to establish a developed method to predict aerodynamic coefficients of the ramjet missiles accurately. Accurate prediction of the aerodynamic coefficients enables the correct calculation of aerodynamic performance values of the configurations. Hereby, missile configurations that truly satisfy the desired aerodynamic performance requirements can be designed initially.

Second objective of this thesis is to perform an inverse design study for a ramjet missile with meta-heuristic optimization algorithms under given geometrical constraints and aerodynamic performance requirements. It has been seen in literature

that there are many types of developed meta-heuristic optimization algorithms used in industry for different purposes. For this study, two commonly used algorithms which are Genetic Algorithm (GA) and Differential Evolution (DE) and one newly developed algorithm which is Modified Cuckoo Search (MCS) are selected to be implemented for design optimization processes. Using these algorithms will surely decrease the time that is spent to find the global optimum configuration in design space by evaluating fewer configurations. Furthermore, a detailed study on the selection of one of the existing optimization algorithms (GA, DE and MCS) is also performed in order to determine the most suitable algorithm for missile configuration design optimization processes.





## CHAPTER 2

### VALIDATION

In this chapter, validation studies are presented for aerodynamic analyses tools and optimization algorithms. First validation is conducted for the aerodynamic analyses tools of Missile DATCOM (MD), Improved Method (MD-imp.) and Fluent. For this purpose, ramjet missile configuration shown in Figure 16 is modeled and analyzed for each tool and then calculated aerodynamic coefficients are compared with experimental data. Second validation is employed for the optimization algorithms. In order to carry out this validation, it is worked on the single-objective optimization problem with selected test function.

#### **2.1 Validation 1: Validation of Aerodynamic Analyses Tools**

Before starting the design optimization process, it is required to validate aerodynamic analyses tools (“MD”, “MD-imp.” and “Fluent”) which are driven to calculate aerodynamic coefficients of missile configurations. For this purpose, missile configuration shown in Figure 16 is analyzed separately with these tools and analysis results have been compared with corresponding experimental data. Validation of the tools has been performed by considering three aerodynamic coefficients:  $C_A$ ,  $C_N$  and  $C_m$ .

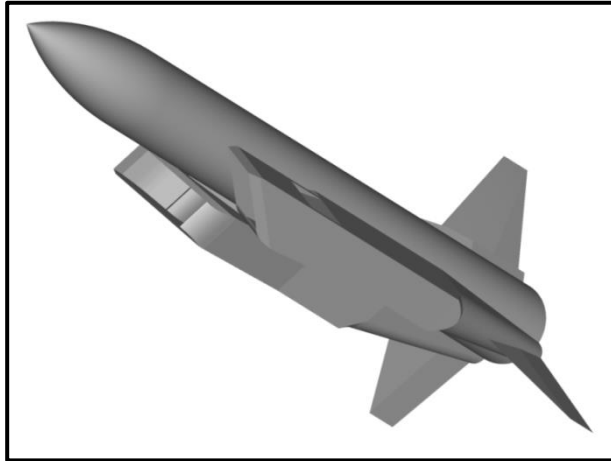


Figure 16: Ramjet missile configuration

The comparative analysis results of the aerodynamic coefficients calculated by available tools can be seen in Figure 17-25. From figures, it is seen that Missile DATCOM (“MD”) analyses results and experimental results are not coherent with each other. On the other hand, Fluent and Improved Method (“MD-imp.”) estimate missile aerodynamic coefficients with better accuracy in comparison to fast prediction tool.

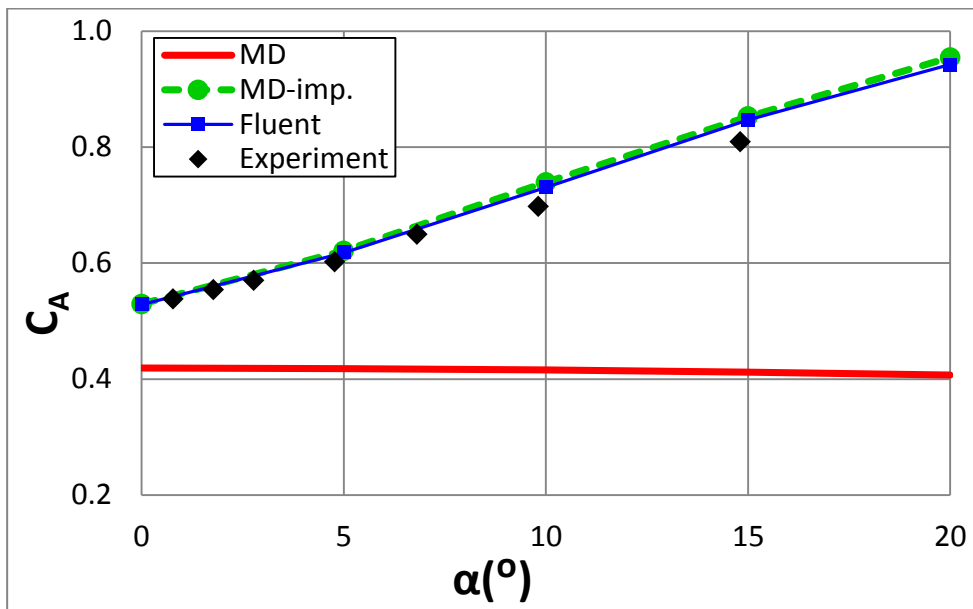


Figure 17: Axial force coefficient validation comparison (Mach=2.5, Re=6.56E+6)

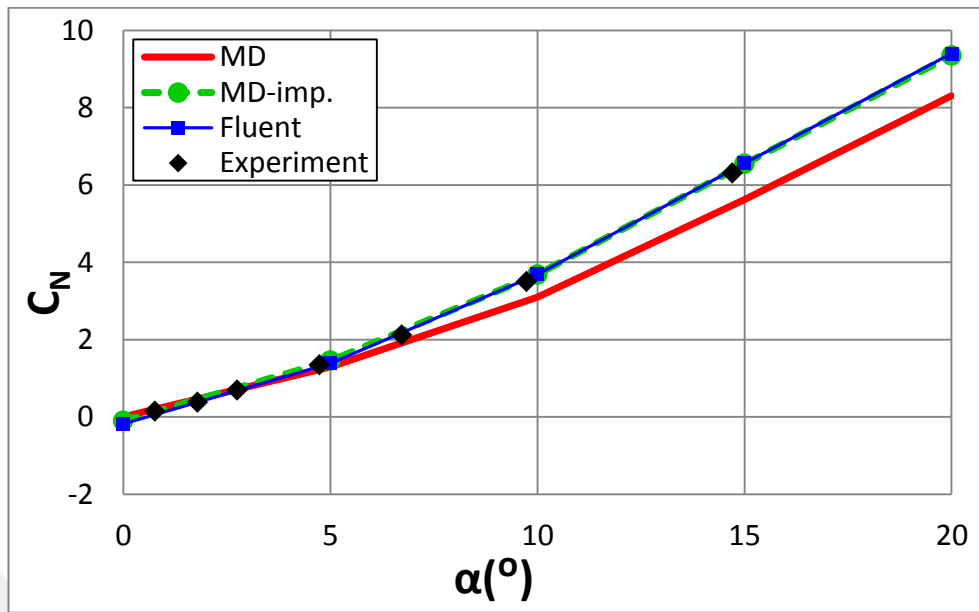


Figure 18: Normal force coefficient validation comparison (Mach=2.5, Re=6.56E+6)

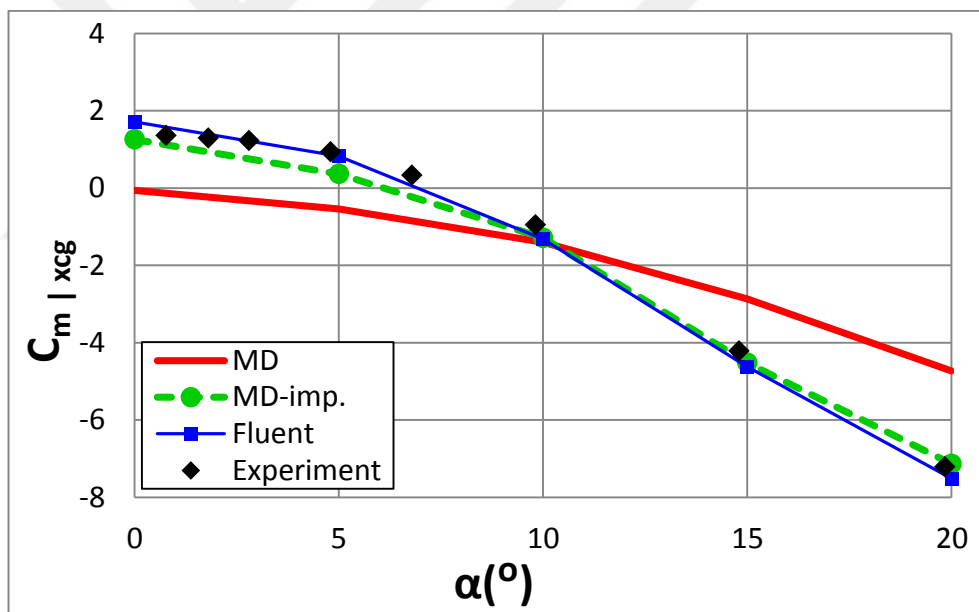


Figure 19: Pitching moment force coefficient validation comparison (Mach=2.5, Re=6.56E+6)

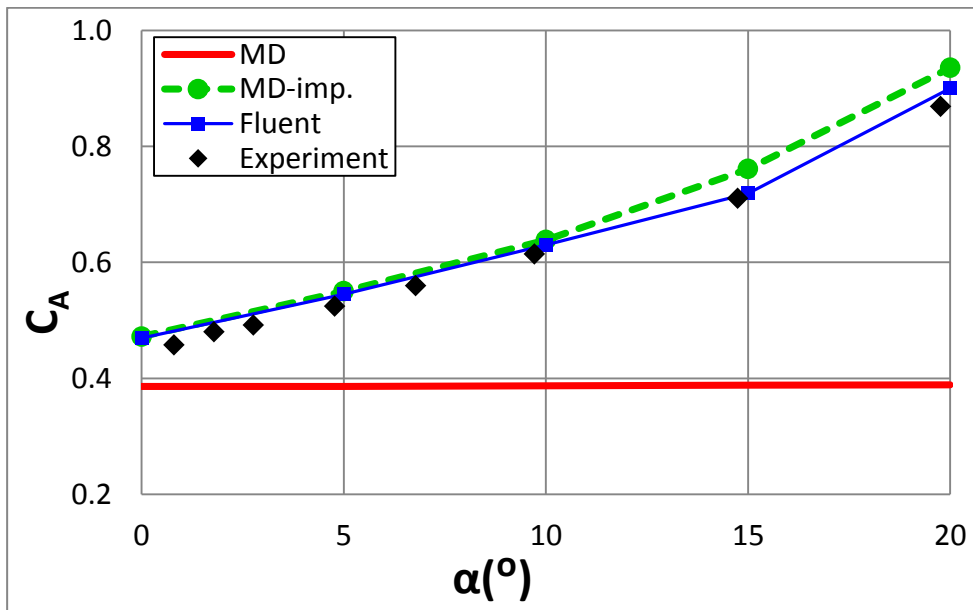


Figure 20: Axial force coefficient validation comparison (Mach=2.95, Re=6.56E+6)

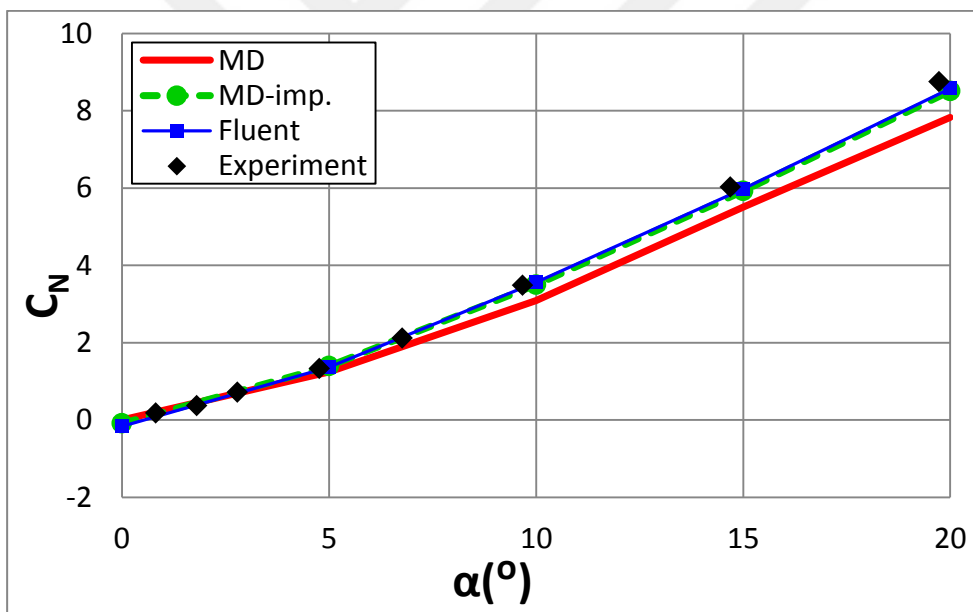


Figure 21: Normal force coefficient validation comparison (Mach=2.95, Re=6.56E+6)

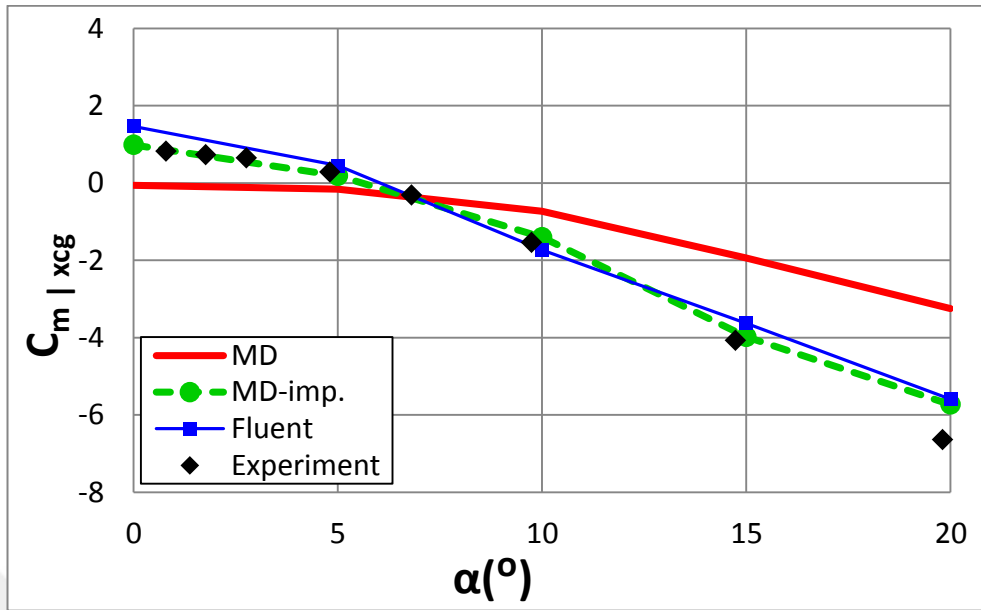


Figure 22: Pitching moment force coefficient validation comparison (Mach=2.95, Re=6.56E+6)

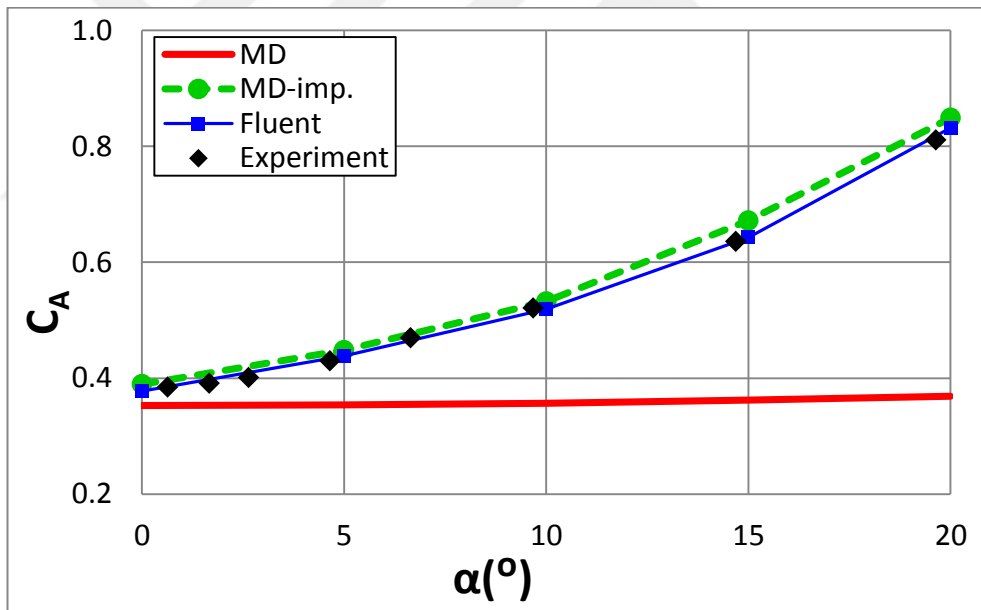


Figure 23: Axial force coefficient validation comparison (Mach=3.5, Re=6.56E+6)

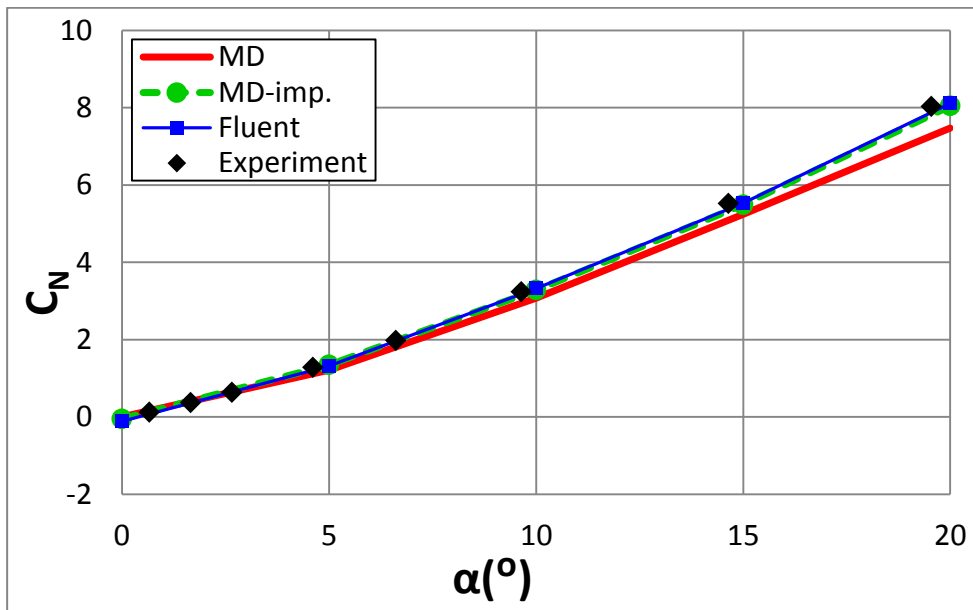


Figure 24: Normal force coefficient validation comparison (Mach=3.5, Re=6.56E+6)

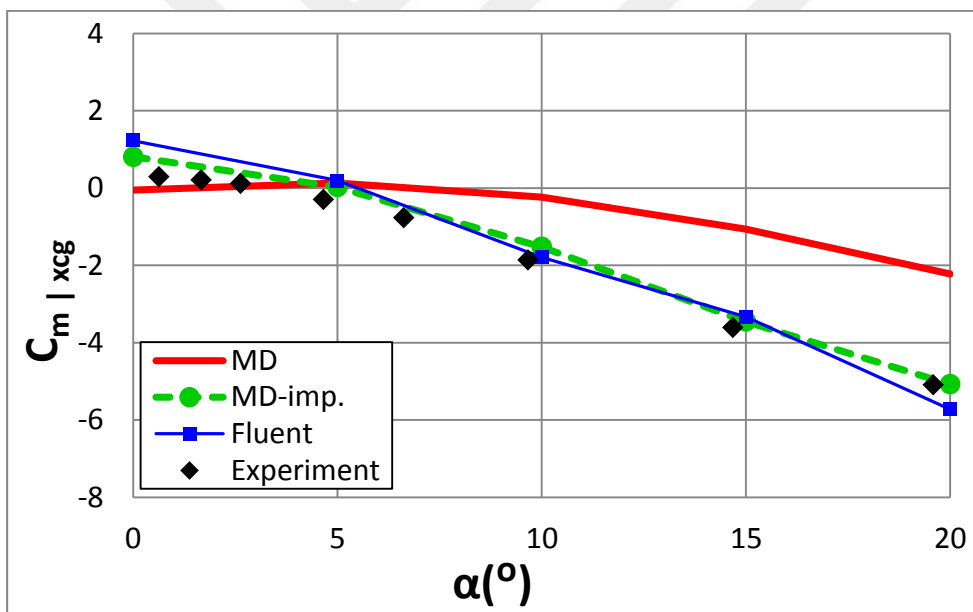


Figure 25: Pitching moment force coefficient validation comparison (Mach=3.5, Re=6.56E+6)

Computational volume grid near the ramjet missile configuration can be seen in Figure 26. Contour plots obtained from Fluent analyses results can be seen in Figure 27-29.

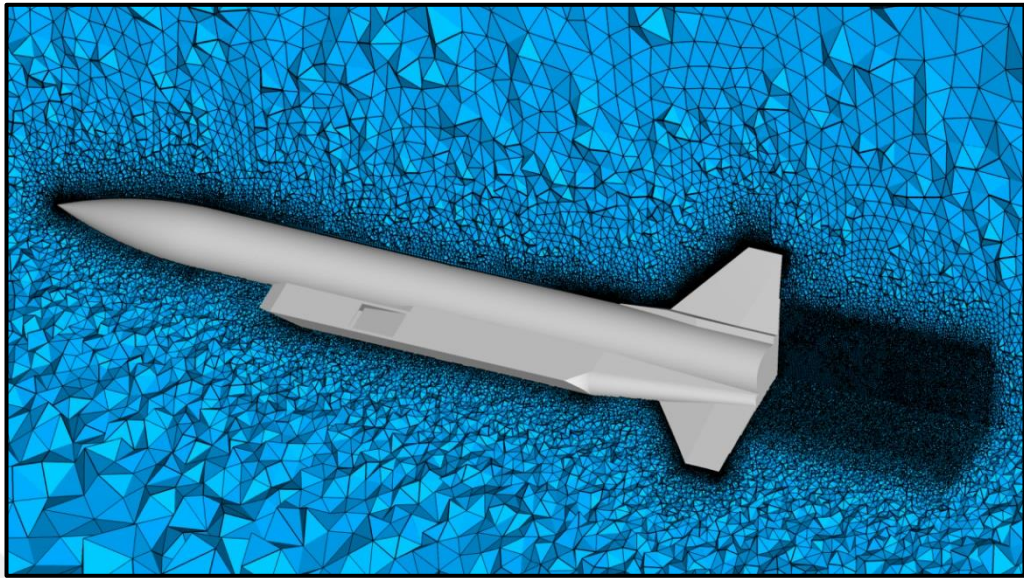


Figure 26: Close view of the computational volume grid

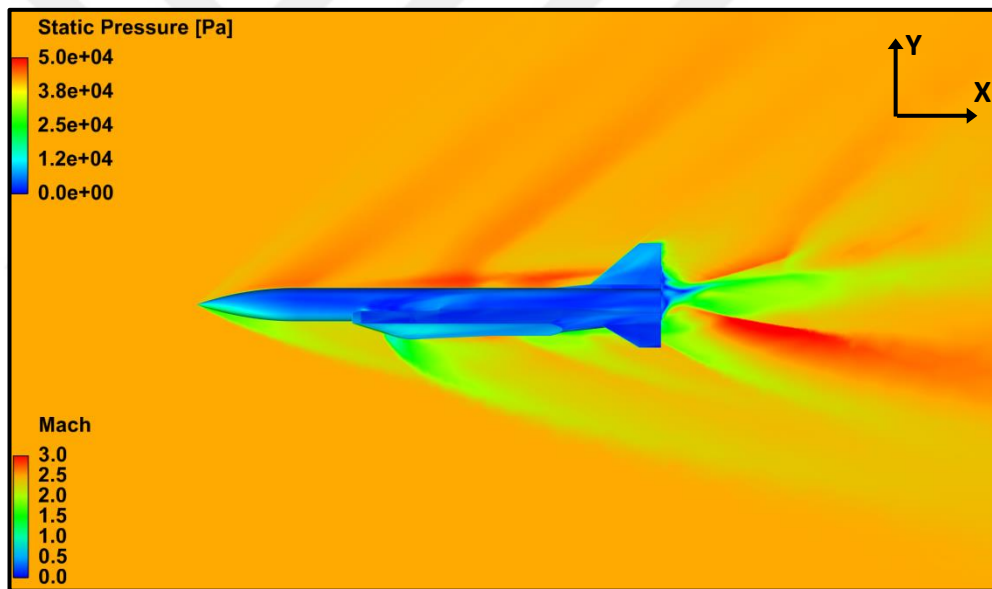


Figure 27: Static Pressure distribution over missile surface and Mach Contour over XY plane (Mach=2.5,  $Re=6.56E+6$ ,  $\alpha=15^\circ$ )

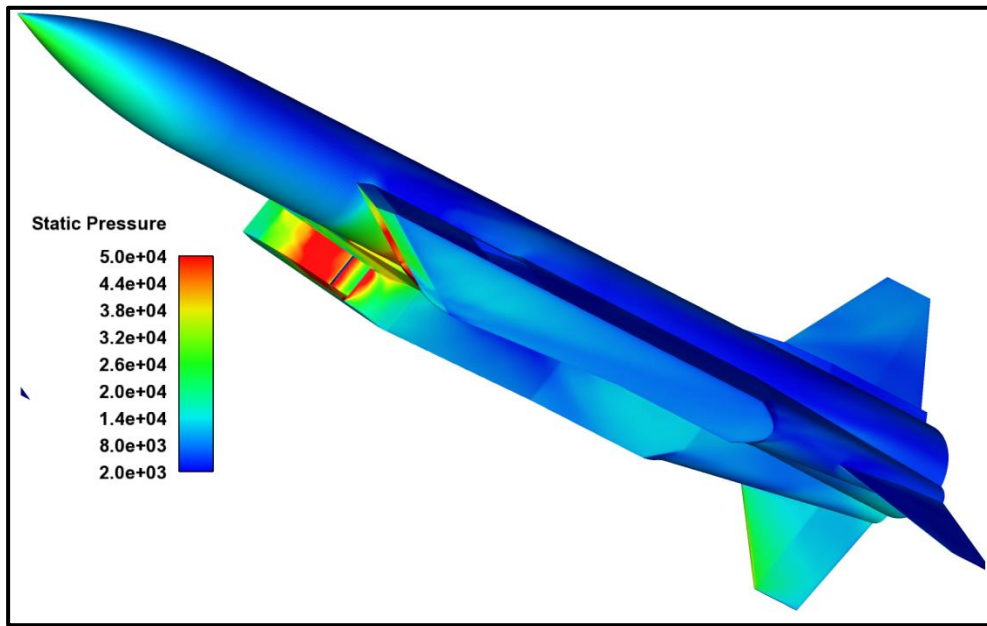


Figure 28: Static Pressure distribution over missile body surface (Mach=2.5, Re=6.56E+6,  $\alpha=15^\circ$ )

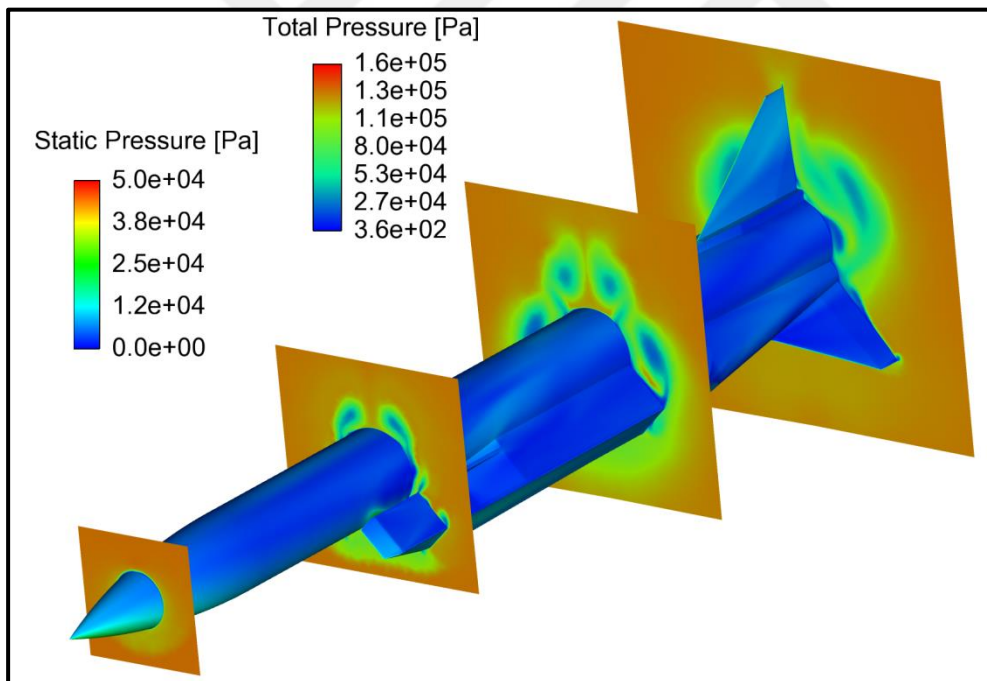


Figure 29: Static Pressure distribution over missile body surface and Total Pressure distribution over cut planes (Mach=2.5, Re=6.56E+6,  $\alpha=15^\circ$ )

## 2.2 Validation 2: Validation of Meta-Heuristic Optimization Algorithms

Validation of the meta-heuristic optimization algorithms which are used in this work is essential to show whether software codes that is written in FORTRAN language work properly or not. For this purpose, Beale Function which is one of the test functions for single-objective optimization problems is selected to be analyzed for each algorithm. During analyses, it is aimed to reach the coordinates of (3.0, 0.5) where Beale Function has global minimum function value of 0.0. Expression of function can be seen in the equation below:

$$f(x, y) = (1.5 + x - xy)^2 + (2.25 + x - xy^2)^2 + (2.625 + x - xy^3)^2$$

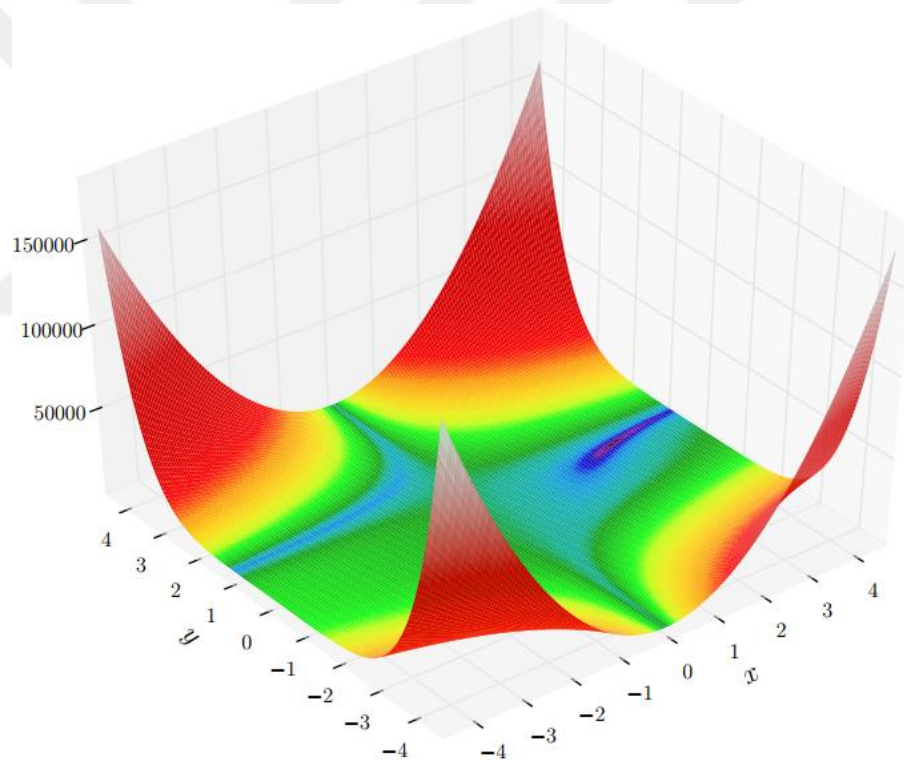


Figure 30: Beale's function plot [23]

Beale function has two variables of x and y. Upper and lower limits of these variables are set to 10.0 and -10.0, respectively.

Analyses of the test function for each algorithm are achieved and results which show decrease in fitness value (evaluated function value) with respect to iteration number

can be seen in Figure 31, 32 and 33. Analyses are repeated for three different initial random numbers (IRN) which are 33857, 12874 and 65871. In addition, population number is set to 20 for all algorithms.

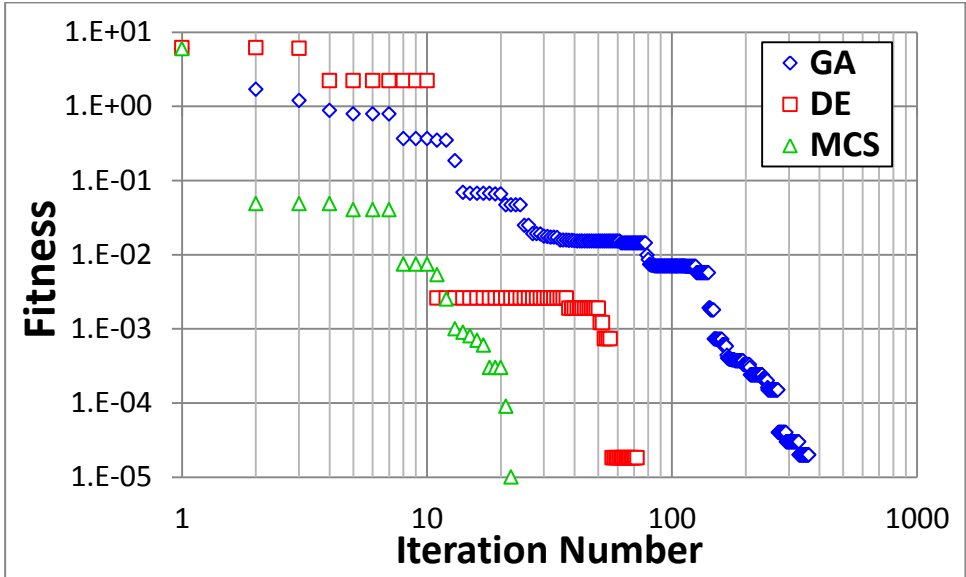


Figure 31 Comparison of fitness values of optimization algorithms (IRN=15685)

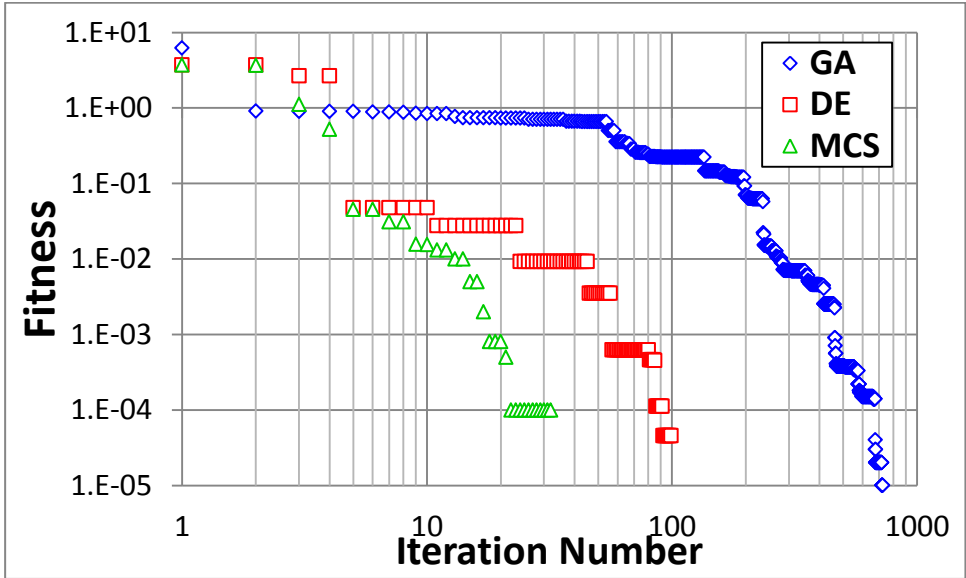


Figure 32 Comparison of fitness values of optimization algorithms (IRN=37329)

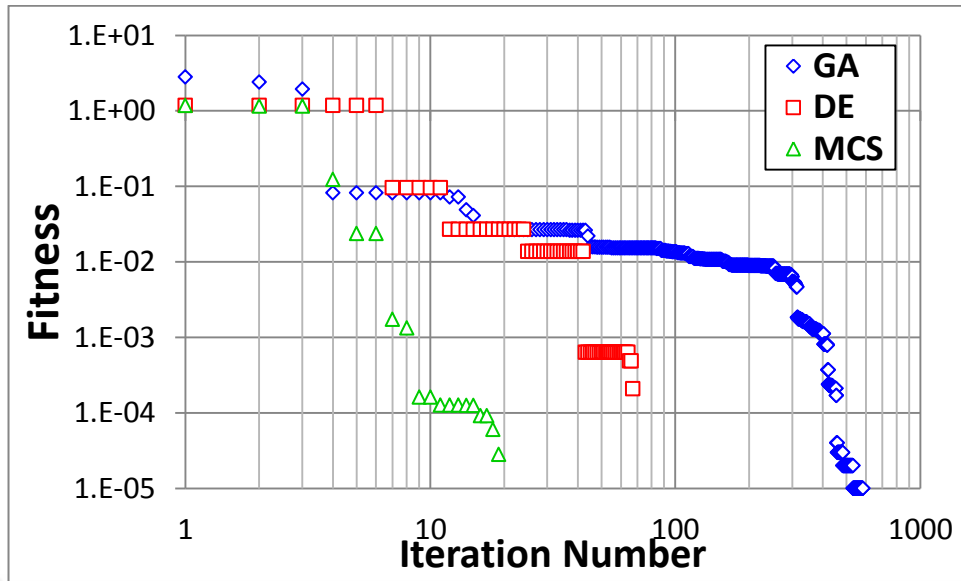


Figure 33: Comparison of fitness values of optimization algorithms (IRN=81653)

Comparison of optimization algorithms concerning their calculated fitness values (referring to evaluated function value) for different initial random numbers are shown in Figure 31, 32 and 33. Y-axes of the plots are set to logarithmic axis making it easier to view the change of fitness values along the X-axes. From figures, it is seen that optimization algorithms have reached the global minimum value of Beale Function at different iteration numbers. Summary of the optimization algorithms regarding their converged iteration numbers can be seen in Table 4.

Table 4: Comparison of optimization algorithms (Iteration Number) with Beale Function

	Iteration Numbers		
	IRN=15685	IRN=55563	IRN=81653
<b>GA</b>	363	725	584
<b>DE</b>	73	100	68
<b>MCS</b>	<b>23</b>	<b>33</b>	<b>20</b>

Table 5: Comparison of optimization algorithms (Function Evaluation Number) with Beale Function

<b>Number of Function Evaluations</b>			
	<b>IRN=15685</b>	<b>IRN=55563</b>	<b>IRN=81653</b>
<b>GA</b>	7260	14500	11680
<b>DE</b>	2900	4020	2700
<b>MCS</b>	<b>536</b>	<b>719</b>	<b>485</b>

In Table 5, numbers of the function evaluations during analyses for each algorithm are summarized. In addition, optimization algorithms of the present study are compared with referenced optimization algorithm (MCS-Ref.) used in the study of Walton [22]. Analyses are carried out for the 10-dimensional version of Rosenbrock's test function. As it is shown in Figure 34, initial Euclidean distance from the global minima are different for the present study and referenced study [22] since corresponding initial populations are different.

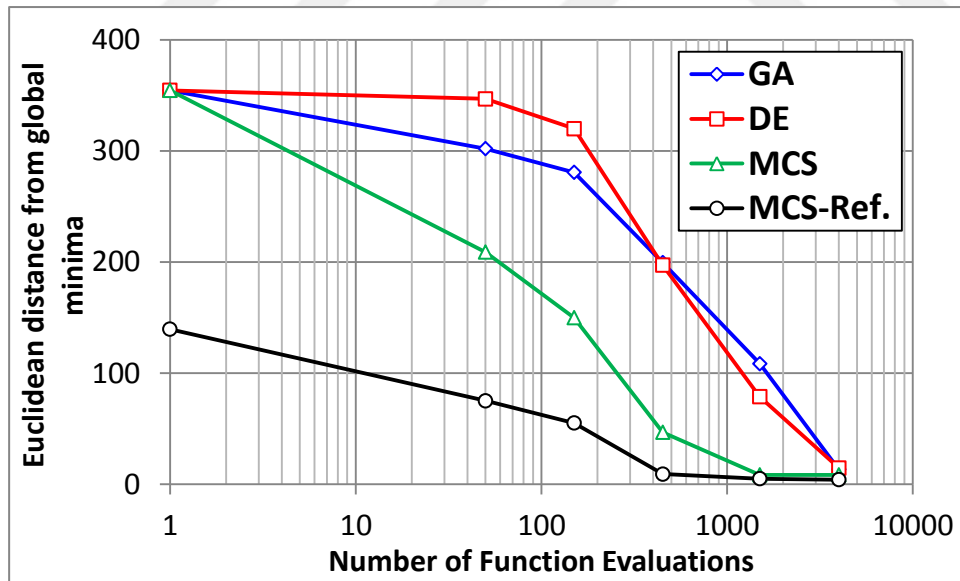


Figure 34: Comparison of optimization algorithms including referenced MCS algorithm with Rosenbrock function (d=10)

As it is shown in Table 4-5, modified cuckoo search algorithm has superior convergence speed when compared to genetic algorithm and differential evolution.

The important feature of the MCS algorithm is the use of Levy Flights to generate new candidate solutions throughout local and global searching. Levy flight is a random walk characterized by a series of instantaneous jumps generated by a probability density function which has a power law tail. Sampling from such distributions results in mostly small values with a few very large valued samples. This random walk strategy, which is frequently found in nature [24], represents the optimum random search pattern.

However, it is not correct to generalize that MCS algorithm is the best algorithm considering its lowest iteration number, since the algorithm efficiency may vary depending on the problem type. In this part, it is shown that each of the correctly written algorithms can be used to find the global minimum value of the test functions for optimization problems.



## CHAPTER 3

### METHODOLOGY

In this chapter, methods used to calculate aerodynamic coefficients of the missile configurations, those are fast prediction method, improved method and Navier-Stokes method (Fluent), will be introduced firstly. Then, metaheuristic optimization algorithms used for inverse design optimization tasks will be elaborated. Optimization algorithms studied in this work are Genetic Algorithm (GA), Differential Evolution (DE) and Modified Cuckoo Search (MCS) algorithm.

#### **3.1 The Fast Prediction Method (Missile DATCOM)**

In preliminary design phase, estimation of aerodynamic coefficients of missile configurations is usually achieved quickly and economically by fast prediction tools. In this study, fast prediction tool aerodynamic analyses are performed with Missile DATCOM which has capability of partially modeling and analyzing air-breathing inlet components.

Missile DATCOM is a semi-empirical fast prediction tool which has predictive accuracy suitable for preliminary design phase of conventional missiles. Solution type of this tool is based on component build up method [25]. In this method, components of the missile are analyzed separately and then all the components and their interferences among each other are combined to obtain aerodynamic coefficients of the complete missile.

The formulations used in component build-up method of Missile DATCOM fast prediction tool to calculate aerodynamic coefficients of missile configurations can be seen in the equations below:

$$C_A = C_{ABA} + C_{AT(B)} + C_{AR} \quad (3.1)$$

$$C_N = C_{NBA} + C_{NB(T)} + C_{NT(B)} + C_{NR} \quad (3.2)$$

$$C_m = C_{mBA} + C_{mB(T)} + C_{mT(B)} + C_{mR} \quad (3.3)$$

where,

$$C_{NB(T)} = \frac{K_{B(T)}}{K_{T(B)}} C_{NT(B)}, \quad C_{mB(T)} = \frac{K_{B(T)}}{K_{T(B)}} C_{mT(B)} \text{ XCPBT}$$

Table 6: Explanation of the subscripts

<b>Symbols</b>	<b>Explanation</b>
BA	Body alone
B(T)	Body in presence of tail (Increment)
T(B)	Tail in presence body
KT(B), KB(T)	Interference factors
XCPBT	Center of pressure of increment force
R	Ramjet

### 3.2 Improvements on Fast Prediction Method (Improved Method)

In this work, it is aimed to model and analyze a missile configuration having air-breathing component which is shown in Figure 35. By considering the results presented in validation part of this study, it is understood that it is necessary to establish a developed method to calculate aerodynamic coefficients of ramjet missiles accurately since the prediction accuracy of engineering level fast prediction tools are not sufficient.

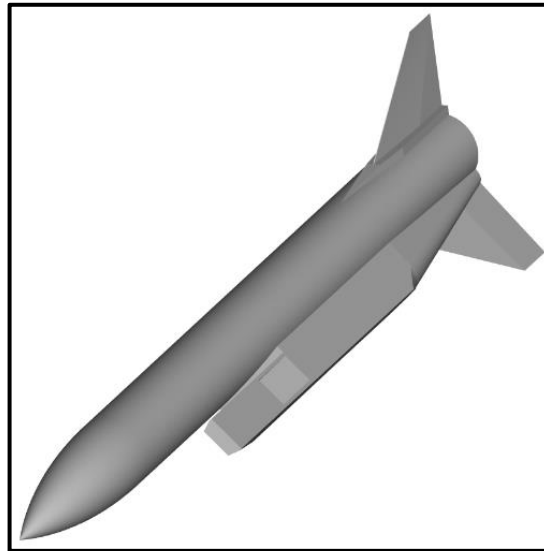


Figure 35: Ramjet missile configuration

The improved method proposed in this work is based on the component build up method [25]. In this improved method, ramjet components and body part of the missile are united and they are considered as a combined body (Body+ Ramjet) as it is shown in Figure 36; whereas they are treated as separated parts in the method of fast prediction tool. On the other hand, there is no difference between improved method and fast prediction method about handling the fin part of the missile configuration which is shown in Figure 37.

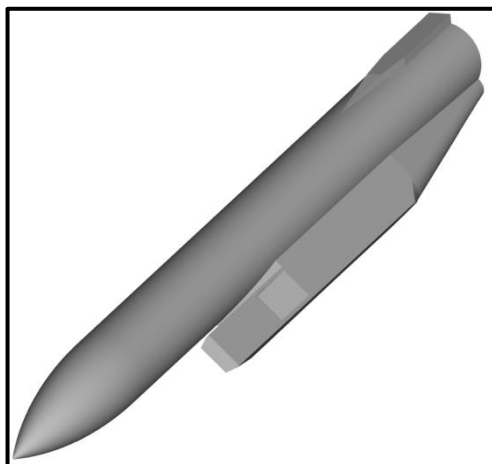


Figure 36: Combined body (Body +Ramjet)

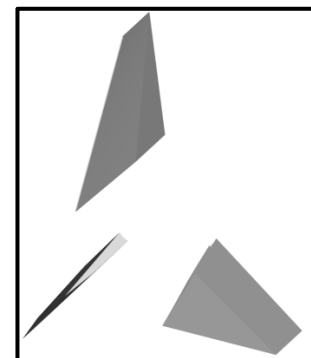


Figure 37: Tail Fin Set

The formulations used in the improved method to calculate aerodynamic coefficients of missile configurations are presented in the equations below:

$$C_A = C_{ABR} + C_{AB(T)} \quad (3.4)$$

$$C_N = C_{NBR} + C_{NB(T)} + C_{NT(B)} \quad (3.5)$$

$$C_m = C_{mBR} + C_{mB(T)} + C_{mT(B)} \quad (3.6)$$

where,

$$C_{NB(T)} = \frac{K_{B(T)}}{K_{T(B)}} C_{NT(B)}, \quad C_{mB(T)} = \frac{K_{B(T)}}{K_{T(B)}} C_{NT(B)} XCPBT$$

Table 7: Explanation of the subscripts

<b>Symbols</b>	<b>Explanation</b>
BR	Body+Ramjet
B(T)	Body in presence of tail (Increment)
T(B)	Tail in presence body
$K_{T(B)}, K_{B(T)}$	Interference factors
XCPBT	Center of pressure of increment force

In the calculation of aerodynamic coefficients with given improved method formulations, Fluent analyses results are used for the terms having “BR” subscript (body contribution). In this way, complex aerodynamic phenomena effects occurring inside the ramjet and interference effects between the ramjet components and missile body are included. On the other hand, remaining terms having “B(T)” and “T(B)” subscripts (fin contribution) are calculated by the help of Missile DATCOM fast prediction tool. Summation of appropriate terms finally gives the complete missile configuration aerodynamic coefficients.

Missile DATCOM fast prediction tool is based on the component build-up method which gives an opportunity to examine missile aerodynamic coefficients on the component basis. This feature of the tool may help to find out why Missile DATCOM has relatively poor prediction accuracy with respect to Fluent and

improved method. Therefore, Missile DATCOM and Fluent analyses results of the missile configuration on the component basis (combined body and tail fin) are compared in Figure 38-43.

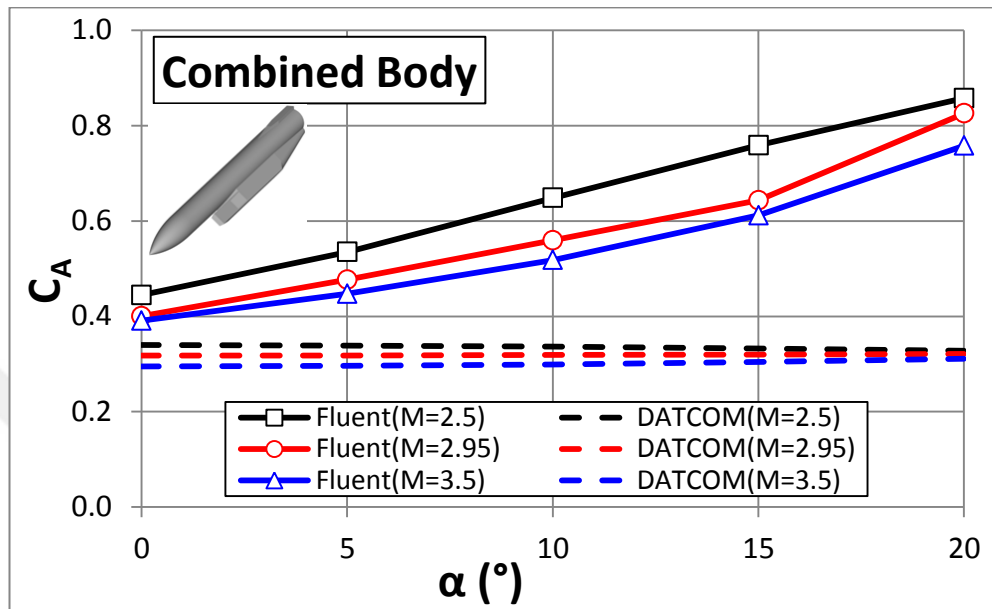


Figure 38: Combined body axial force coefficient validation comparison (Re=6.56E+6)

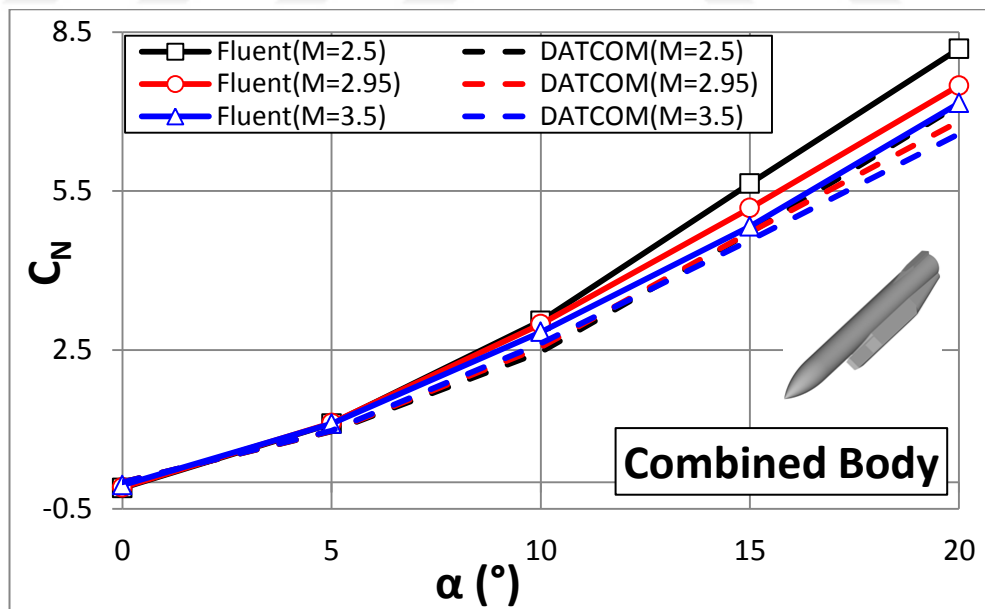


Figure 39: Combined body normal force coefficient validation comparison (Re=6.56E+6)

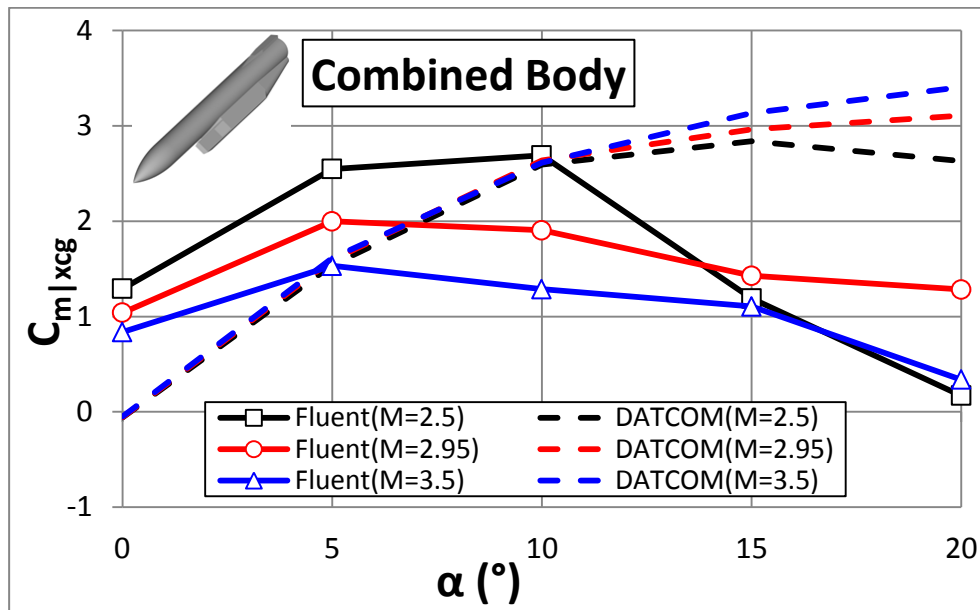


Figure 40: Combined body pitching moment coefficient validation comparison (Re=6.56E+6)

According to Figure 38-40, Missile DATCOM and Fluent analyses results regarding to static aerodynamic coefficients ( $C_A$ ,  $C_N$ ,  $C_{m|xcg}$ ) of the combined body component are not coherent with each other. Therefore, it can be understood that it is essential to use Fluent analyses results for the combined body component by considering the consistency of Fluent analyses results with experimental data where it is shown Figure 17-25.

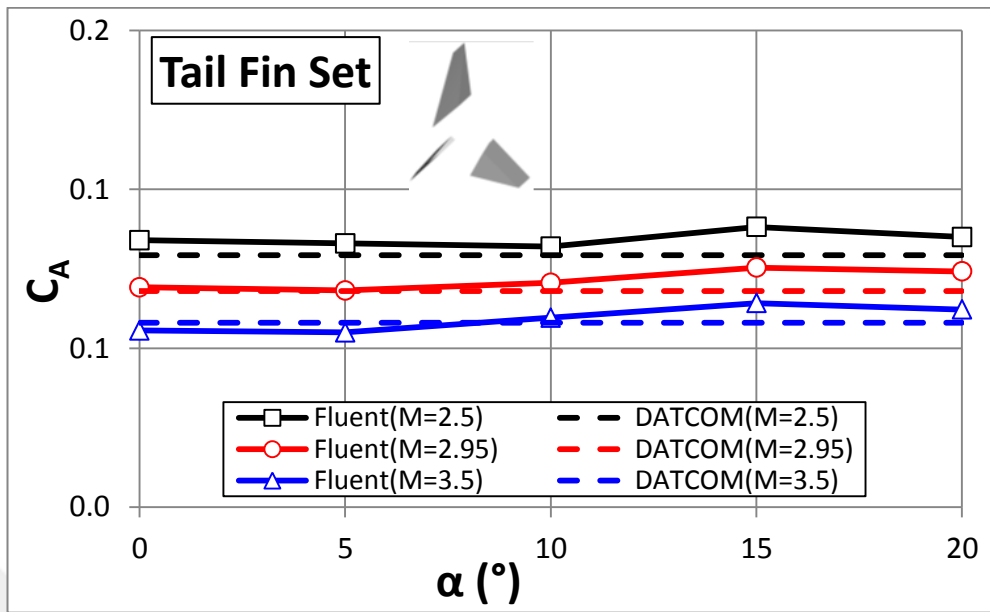


Figure 41: Tail fin axial force coefficient validation comparison (Re=6.56E+6)

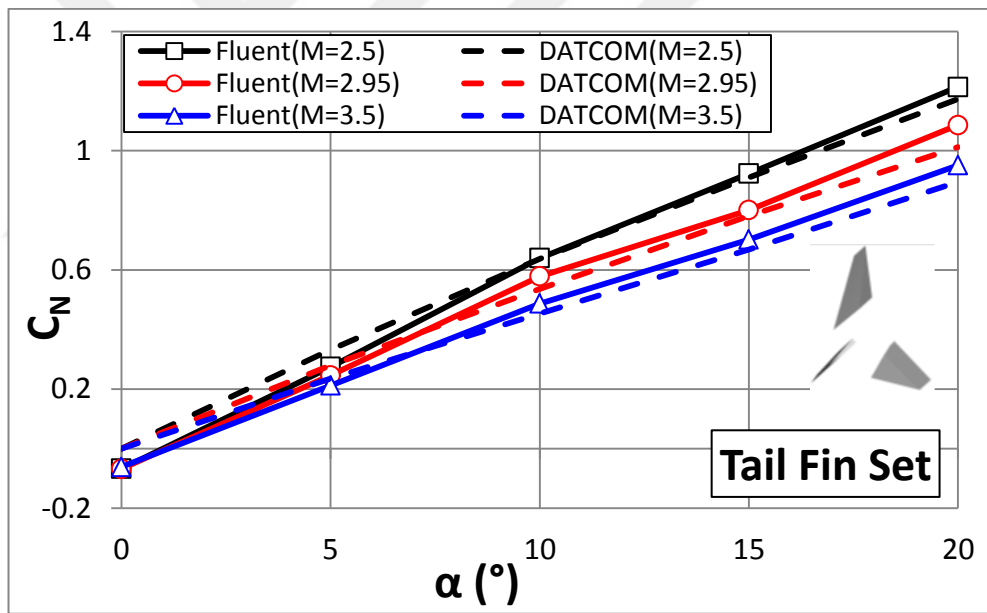


Figure 42: Tail fin normal force coefficient validation comparison (Re=6.56E+6)

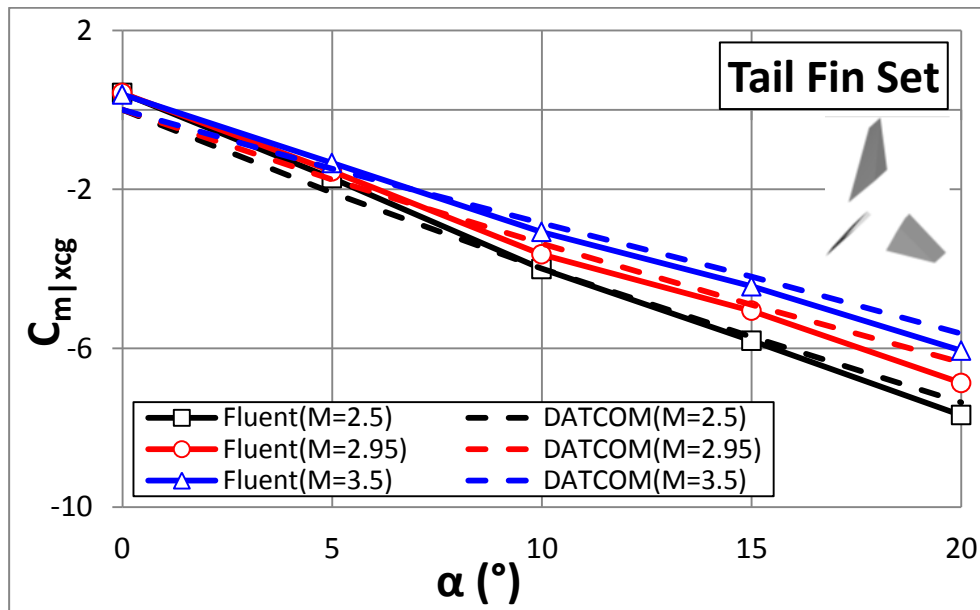


Figure 43: Tail fin pitching moment coefficient validation comparison (Re=6.56E+6)

Similar analyses are also conducted for the tail fin set component of the missile configuration and calculated aerodynamic coefficients are presented in Figure 41-43. From figures, it is seen that Missile DATCOM prediction accuracy for tail fin set component aerodynamic coefficients is acceptable. It is of importance to use Missile DATCOM for analyses of the tail fin set component as it will significantly reduce the optimization time of the design optimization tasks.

Interference factors ( $K_{T(B)}$ ,  $K_{B(T)}$ ) also contribute the calculation of the missile aerodynamic coefficients. Formulations of these factors are:

$$K_{B(T)} = \frac{C_{N_{B(T)}}}{C_{N_T}}, \quad K_{T(B)} = \frac{C_{N_{T(B)}}}{C_{N_T}}$$

Comparisons of interference factors obtained from Missile DATCOM and calculated by using Fluent analyses results can be seen in Figure 44 and 45:

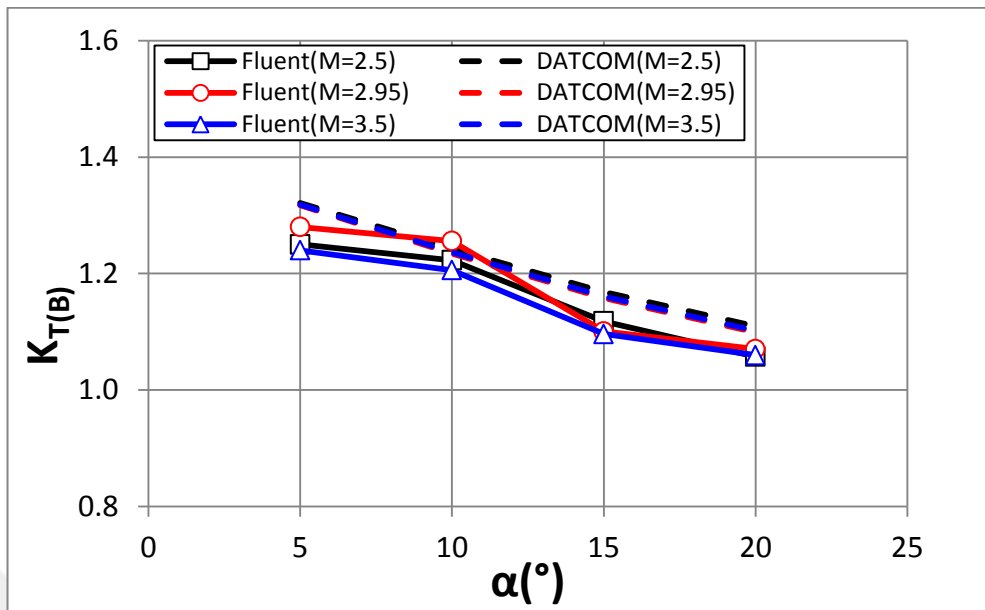


Figure 44: Comparison of computed tail in the presence of body interference factors

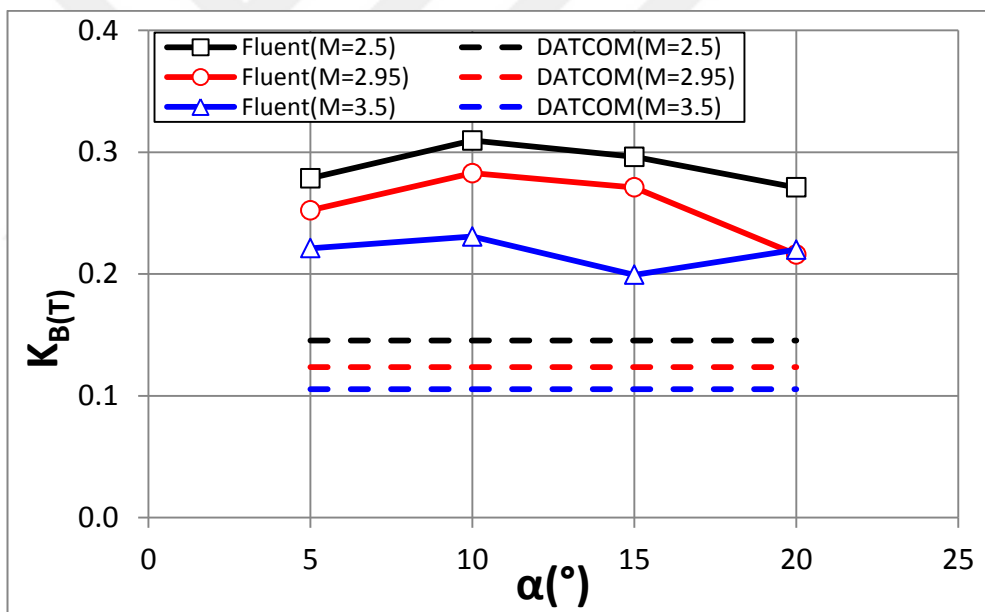


Figure 45: Comparison of computed body in the presence of tail interference factors

From Figure 44, it is understood that there is somewhat coherency between Missile DATCOM and Fluent  $K_{T(B)}$  interference factors. On the other hand, in Figure 45, it is seen that Missile DATCOM and Fluent  $K_{B(T)}$  interference factors are not coherent with each other.

Since the calculation of the interference factors are highly geometry dependent, it is essential to examine the effect of other geometric parameters on these factors. Therefore, the behavior of the interference factors with respect to missile body diameter (D), tail span (Span) and tail leading edge position (LE) are investigated with both the fast prediction and Navier-Stokes method and comparative results are presented in Figure 46-51.

The behavior of the interference factors with respect to missile body diameter (D) can be seen in Figure 46 and 47.

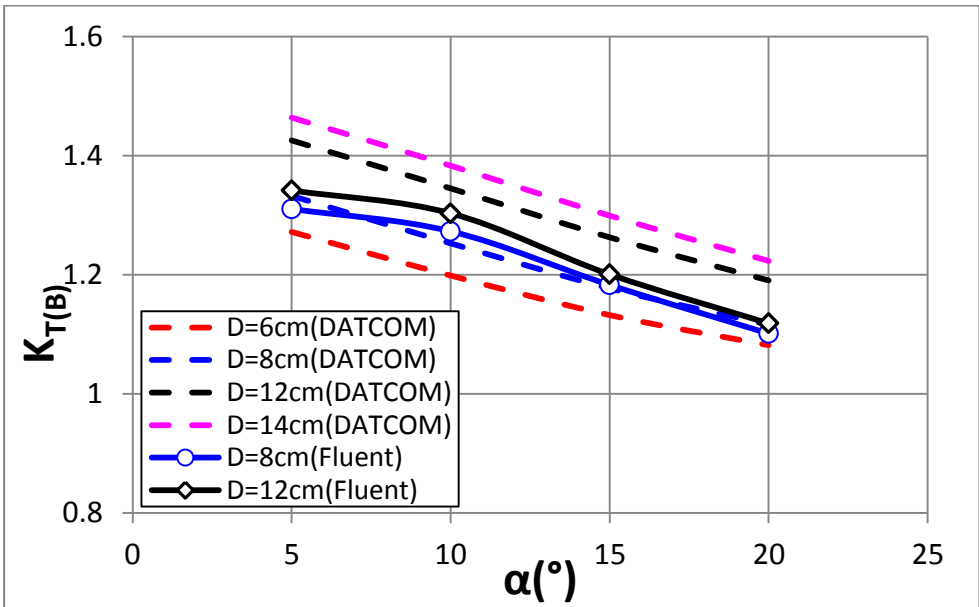


Figure 46: Variation of tail in the presence body interference factors with respect to different missile body diameters (M=2.5)

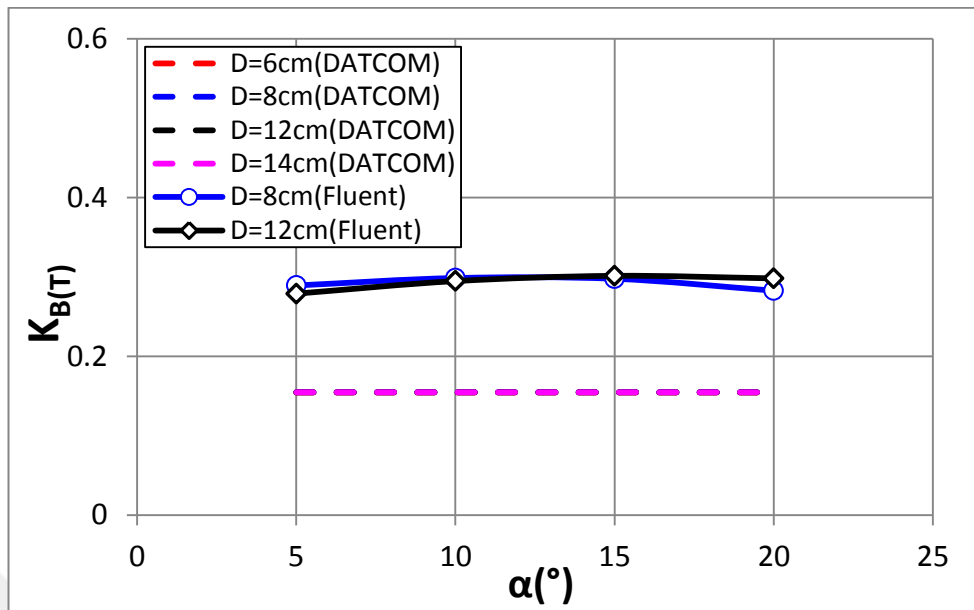


Figure 47: Variation of body in the presence tail interference factors with respect to different body diameters ( $M=2.5$ )

From Figure 46, it is seen that both DATCOM and Fluent  $K_{B(T)}$  interference factor values increase with increasing body diameter. On the other hand, in Figure 47, both Missile DATCOM and Fluent  $K_{T(B)}$  interference factor values seem to be almost insensitive to body diameter change.

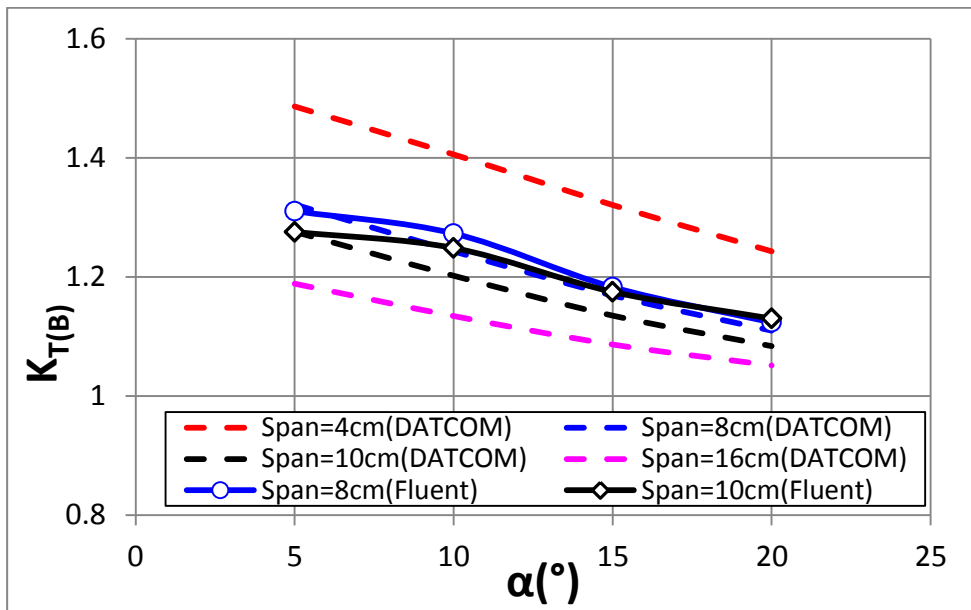


Figure 48: Variation of tail in the presence body interference factors with respect to different span values ( $M=2.5$ )

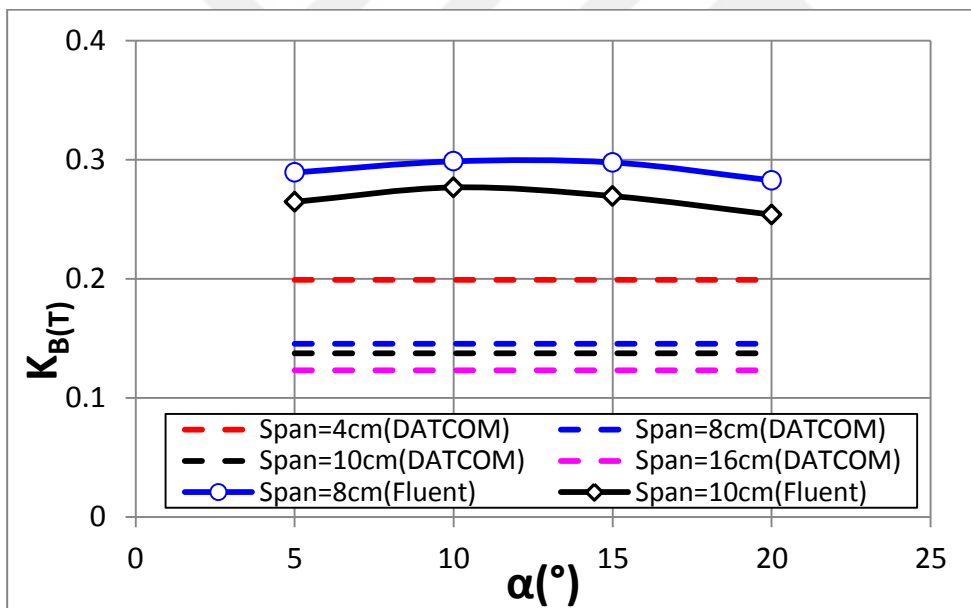


Figure 49: Variation of body in the presence tail interference factors with respect to different span values ( $M=2.5$ )

The behavior of the interference factors with respect to tail fin span value can be seen in Figure 48 and 49. As it is seen from the figures, both interference factors are inversely proportional to tail fin span value.

Analyses for different tail fin set leading edge positions (XLE) are also achieved and results are presented in Figure 50 and 51. From figures, it can be deduced that  $K_{B(T)}$  interference factor is strongly dependent on leading edge position, unlike the  $K_{T(B)}$  interference factor. The reason of the  $K_{B(T)}$  interference factor strong leading edge dependency is that interacted body portion behind the tail fin set is increased as leading edge position moves to forward (being closer to nose).

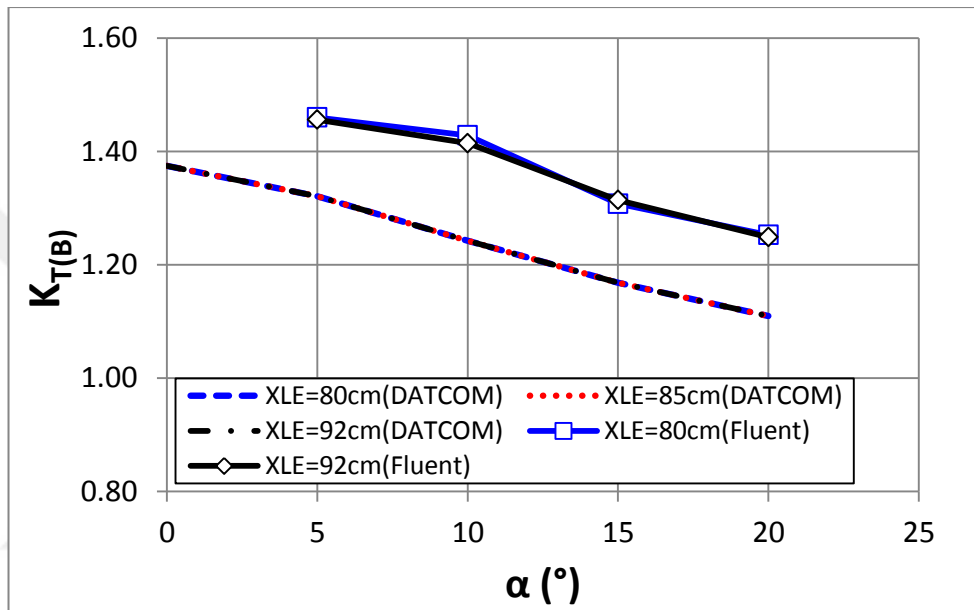


Figure 50: Variation of tail in the presence body interference factors with respect to different leading edge positions (M=2.5)

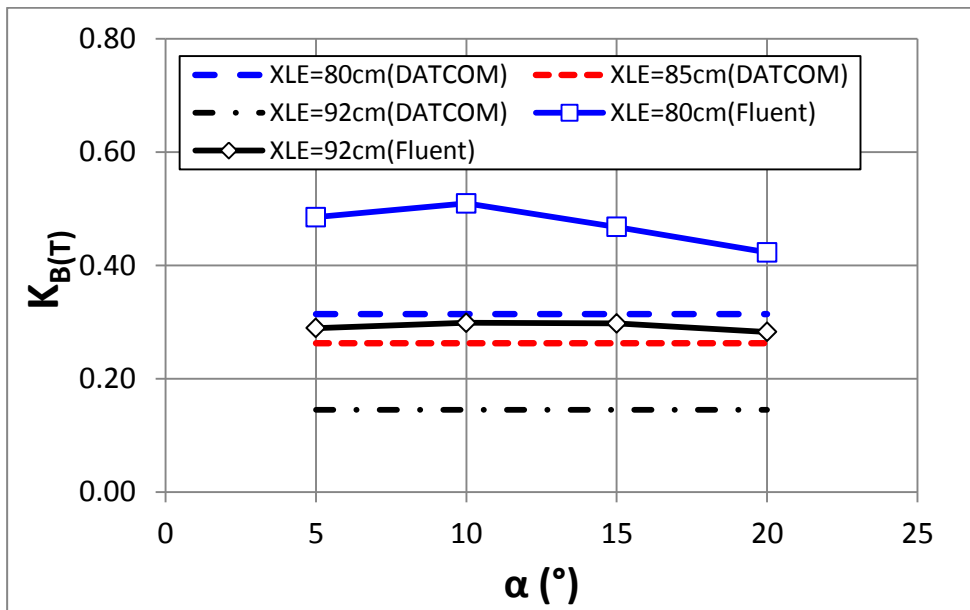


Figure 51: Variation of body in the presence tail interference factors with respect to different leading edge positions ( $M=2.5$ )

After evaluating the analysis results of the interference factors, it can be concluded that, unlike the  $K_{T(B)}$  interference factor, it is important to modify the  $K_{B(T)}$  interference factor benefiting from the Fluent analyses.

Error analysis comparison of the aerodynamic coefficients calculated with Missile DATCOM and Fluent interference factors can be seen in Figure 52-57. From figures, it can be deduced that prediction accuracy for the normal force coefficient and pitching moment coefficient is improved by using interference factors calculated from Fluent instead of Missile DATCOM (MD).

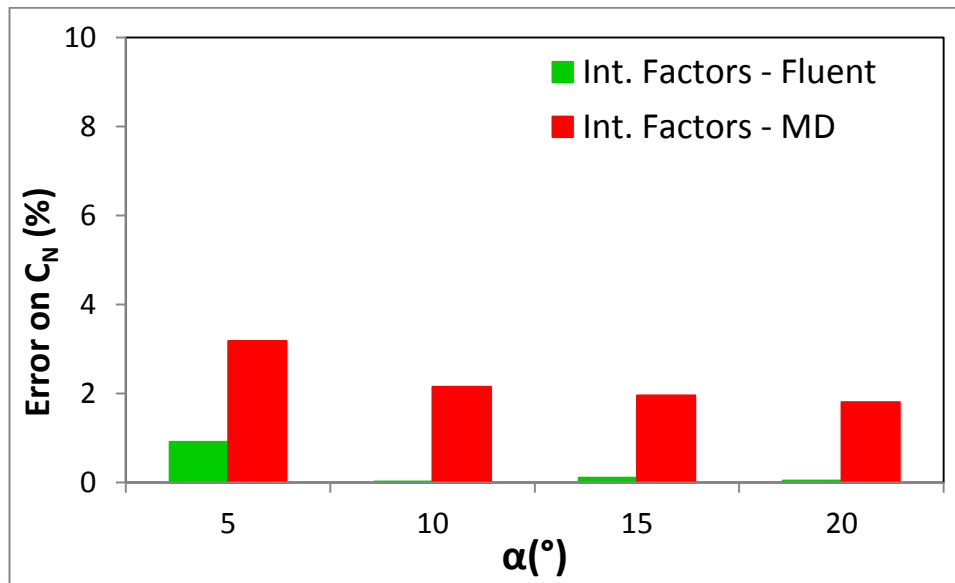


Figure 52: Percentage error analyses of  $C_N$  calculated with MD and Fluent Interference Factors ( $M=2.5$ )

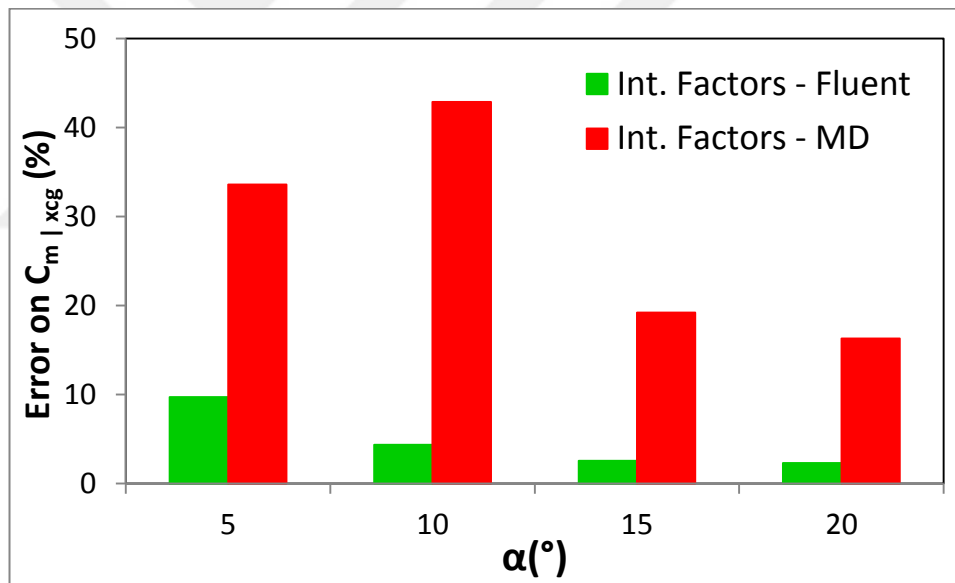


Figure 53: Percentage error analyses of  $C_{m|x_{cg}}$  calculated with MD and Fluent Interference Factors ( $M=2.5$ )

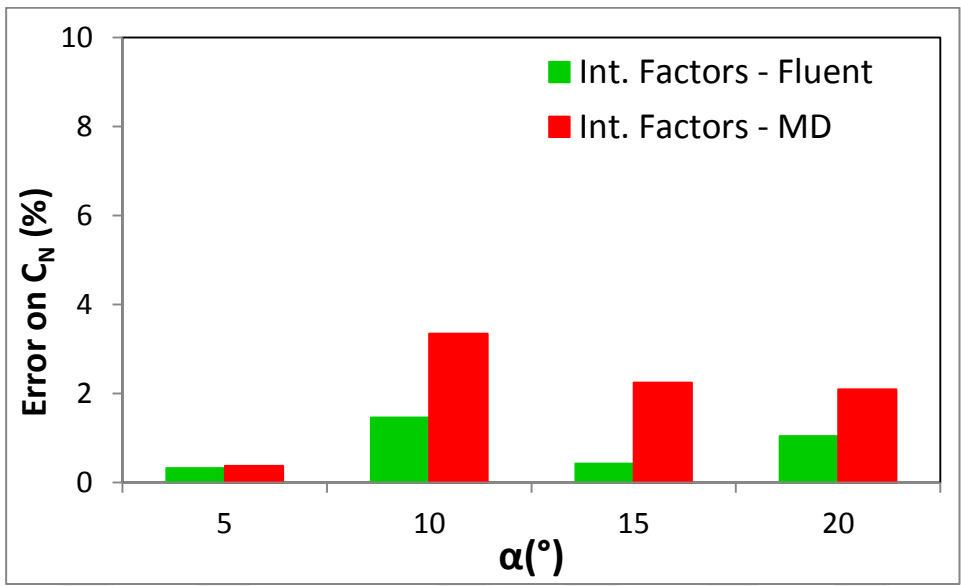


Figure 54: Percentage error analyses of  $C_N$  calculated with MD and Fluent Interference Factors ( $M=2.95$ )

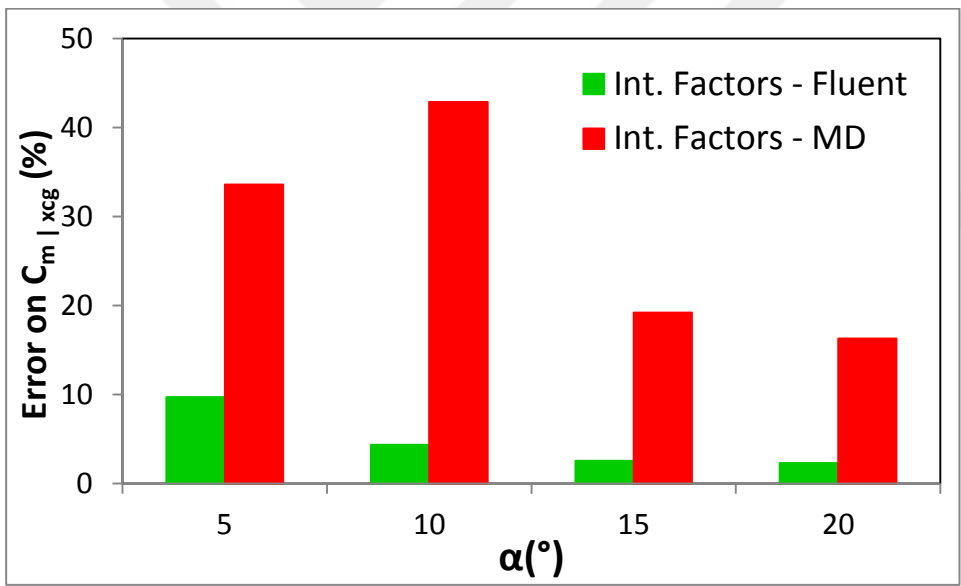


Figure 55: Percentage error analyses of  $C_{m|x_{cg}}$  calculated with MD and Fluent Interference Factors ( $M=2.95$ )

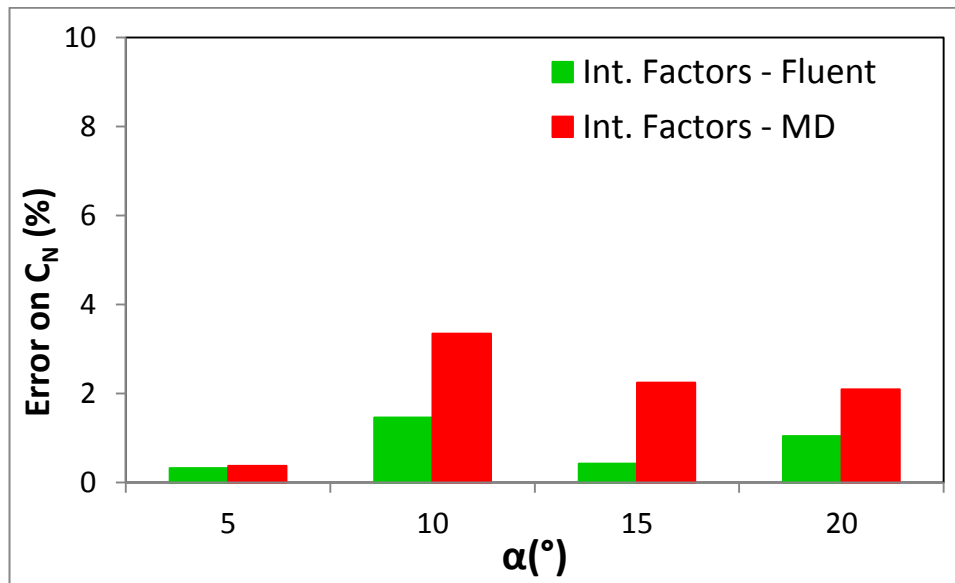


Figure 56: Percentage error analyses of  $C_N$  calculated with MD and Fluent Interference Factors ( $M=3.5$ )

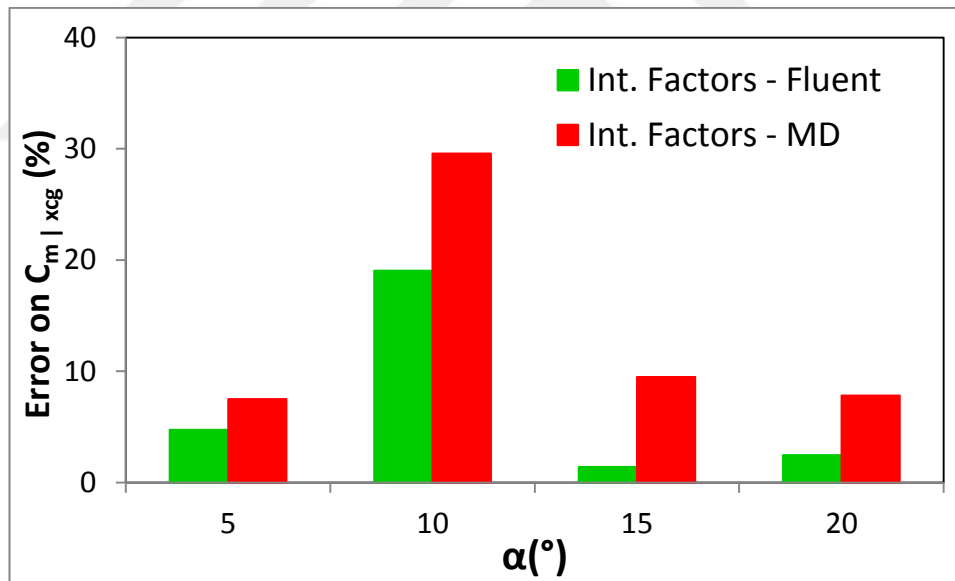


Figure 57: Percentage error analyses of  $C_{m|x_{cg}}$  calculated with MD and Fluent Interference Factors ( $M=3.5$ )

### **3.3 CAD, Grid Generator, CFD and Post Processing Tools**

Ramjet missile configurations can be modeled/meshed in detail and analyzed to have better solutions by the help of the CAD/grid generator and CFD Analysis tools, respectively. In this study, it is benefitted from the Solidworks Computer Aided Drawing (CAD) tool to model in detail ramjet missile configuration. Then, the meshing procedures are implemented on the output model of the CAD tool by the help of Gambit and TGrid grid generation tools. Next, prepared detailed meshed model is used in order to achieve CFD analyses benefiting from the ANSYS Fluent Tool. Finally, computed data is postprocessed by means of the Tecplot and Enight Tools.

During the CAD model preparation, it is endeavored to include all geometrical details as far as possible by considering the ramjet missile configuration geometry available in the study of Hayes [4]. For this prepared detailed CAD model, grid density of fluid domain near the components of the missile configuration, especially for the inlet component, is preferred to be denser when compared to grid density of other conventional missile configurations. With appropriate meshed model, the Fluent Tool configuration is altered to density based solver with energy equation at the beginning of the solution stage. Throughout the solution stage, the turbulence parameters and Courant number are changed appropriately as iteration number increases.

Selection of the turbulence model is also key issue for the numerical analyses to include random or chaotic nature of turbulence phenomena. Turbulence modeling approaches can be mainly categorized under three headings: Reynolds Averaged Navies Stokes (RANS), Large Eddy Simulation (LES) and Direct Numerical Simulation (DNS).

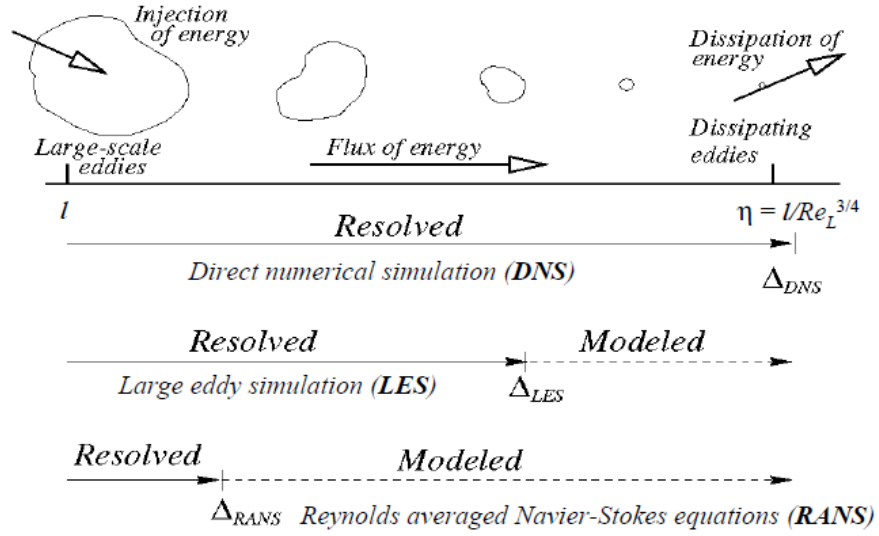


Figure 58: Comparison of turbulence models [26]

In Direct Numerical Simulation (DNS), the Navier-Stokes equations are solved on a sufficiently fine grid to be able to fully resolve all length and time scales and it requires immense computer resources. High computational cost of the DNS can be decreased to some level by applying a filter on small scales with Large Eddy Simulation (LES). In LES, unsteady simulations of fluid flow are achieved by resolving and modeling large and filtered small eddies, respectively.

Reynolds Averaged Navier Stokes (RANS) is preferable for industrial applications since it is the most practical and computationally friendly method for turbulence modelling. In RANS method, instantaneous variables such as velocity, pressure are decomposed into mean and fluctuating value as follows [27]:

$$U_i = \bar{U}_i + u_i \quad (3.1)$$

$$P = \bar{P} + p_i \quad (3.2)$$

In RANS method, variables in the Navier-Stokes equations are altered with their mean and fluctuating terms and then it is tried to model contribution of the fluctuation variables to the change of the averaged ones.

There are many RANS turbulence modelling methods used in industry through different applications. In this study, realizable k- $\epsilon$  (two equation model) [28] is selected as the turbulence model to be used in numerical analyses.

Realizable k- $\epsilon$  turbulence model differs from the standard k- $\epsilon$  model with new model of dissipation rate equation and a new realizable eddy viscosity formulation. New model with a set of unified model coefficients perform well for:

- i. Rotating homogenous shear flows.
- ii. Boundary-free shear flows including a mixing layer, planer and round jets.
- iii. Channel flow, and flat plate boundary layer with and without a pressure gradient.
- iv. Backward facing step separated lows.

Strength of the realizable k- $\epsilon$  turbulence model for external flow problems is also proven with comparison study for flow over a wall-mounted square cylinder [29].

### 3.4 Optimization Algorithms

In this part, details of the optimization algorithms are summarized in the following sub-headings.

#### 3.4.1 Cuckoo Search Algorithm

Cuckoo search meta-heuristic optimization algorithm which is offered by Yang and Deb in 2009 is inspired from the way of regeneration of the host bird nests' against parasitic intruders (cuckoo birds) and how they co-evolve together if invasion takes place. Broadly, the idea is based upon how cuckoo eggs are laid in the host nests, how hosts hatched the eggs (if not detected), how the cuckoo chicks later participate the population of cuckoos and how all of these can be represented mathematically to search for global optimum of a function.

This algorithm can be summarized in four steps as following:

1. A single egg is laid into a randomly chosen host-nest by each cuckoo.
2. The nests with better quality eggs, if not detected, would be hatched to be the cuckoo chicks, who would participate the next generation.
3. The alien egg can be noticed by the host with a probability  $[0,1]$ . If the egg is detected, the host will either destroy the egg or abandon the nest in order to build a new nest elsewhere.
4. When generating new solutions  $x_i^{t+1}$  from old one  $x_i^t$ , Levy flight is performed.

Mathematical representation of generation of new solution from the old one with Levy flight:

$$x_i^{t+1} = x_i^t + \alpha \circ Levy(\beta)$$

where;

$$1 < \beta < 3, \quad \alpha = O(1), \quad \circ = \text{entry - wise multiplication}$$

Algorithm of the original cuckoo search:

---

*Initialization of host nests by laying eggs*  
*Evaluation of the fitness of each egg placed into host nests*  
**do** iteration=1, maximum\_iteration  
    *generate cuckoo eggs by using levy flight from randomly chosen host egg*  
    *evaluate fitness of the cuckoo eggs*  
    *select a random host nest*  
    **if** (fitness of cuckoo egg < fitness of randomly selected host nest egg) **then**  
        *replace host nest egg with cuckoo egg*  
    **end if**  
    **if** (cuckoo eggs are detected) **then**  
        *host will destroy or abandon the nest*  
    **end if**  
    *generate new eggs for the destroyed/abandoned nests*  
    *calculate the fitness for new eggs*  
**end do**

---

### 3.4.2 Modified-Cuckoo Search Algorithm

Modified form of the cuckoo search algorithm [22] differs from the original one with mainly two aspects. First aspect is modification implemented on the Levy flight coefficient of  $\alpha$ . This coefficient refers to constant value of 1 (one) for the original case. In Modified Cuckoo Search, value of  $\alpha$  is a function of the generation number, which will provide more localized searching to get closer solutions as generation number increases. Second aspect is modification employed to prevent repetition of ineffective flights at each generation. For this, crossover over between the solutions has been added to code. Crossover has been applied by changing the structure of the original algorithm.

For a given problem, number of function evaluation is directly related with convergence speed which is crucial for the functions taking a long evaluation time. In this study modified-cuckoo search algorithm which is proposed by Walton in 2013

is employed due to its improved convergence speed when compared to original cuckoo search algorithm.

Value of  $\alpha$  is calculated with following formula in modified cuckoo search algorithm:

$$\alpha = \frac{A}{\sqrt{G}}, \text{ where } A = 1, \quad G = \text{generation number}$$

To prevent reiteration of the ineffective flights, the structure of the algorithm is reconstructed to enable the missing ingredients between the solutions with crossover.

The structure of the Modified-Cuckoo Search algorithm [22] can be seen on the next page.

---

*Initialization of host nests by laying eggs*

*Evaluation of the fitness of each egg placed into host nests*

*G=1*

**do** *G=1, maximum\_generation*

*G=G+1*

*Perform descending sort of the eggs*

*Determine the eggs to be abandoned/destroyed ( 75 % )*

*! (Number of elite eggs= X)*

*! (Number of elite eggs to be abandoned = Number of eggs-X)*

**do** *i=X, Number of eggs*

*stepsize = A/(G<sup>0.5</sup>)*

*Perform levy flight from current egg (ce) to generate new egg (ne)*

*Replace current egg with new egg (ce=ne)*

*Calculate fitness of new egg*

**end do**

**do** *i=1, X*

*current egg (ce) =i*

*select new egg (ne) randomly from elite eggs*

**if** *(ce=ne) then*

*stepsize = A/(G<sup>2</sup>)*

*generate new egg (ne') from current egg (ce)*

*calculate fitness of ne'*

*select new egg (ne'') randomly from all eggs*

**if** *(fitness of ne'' > fitness of ne')* **then**

*ne''=ne'*

**end if**

**else**

*dx=|ce-ne|/(Golden Ratio)*

*generate new egg (ne') adding dx to better one between ne and ce*

*select new egg (ne'') randomly from all eggs*

**if** *(fitness of ne'' > fitness of ne')* **then**

*ne''=ne'*

**end if**

**end if**

**end do**

**end do**

---

### 3.4.3 Differential Evolution

Differential evolution algorithm is proposed by Price and Storn in 1995. In this evolutionary algorithm, population members (solutions) are represented by the vectors of real numbers. Population members are determined randomly if it is known nothing about the system at the beginning of the resolution process, and members of population are evaluated for their fitness values. Then, to generate new trial vector (candidate solution) for each population member, it is utilized randomly selected three different members from existing population.

There are different types of schemes which are used to determine the trial vectors. In this study, it is benefitted from the below scheme which can be explained as:

For each vector  $x_i$ ,  $i = 1, 2, \dots, NP$ , trail vector  $v$  is generated by:

$$v = x_{r1} + \beta \cdot (x_{r2} - x_{r3})$$

where  $r1, r2, r3 \in [1, NP]$ , integer and mutually different,  $\beta > 0$

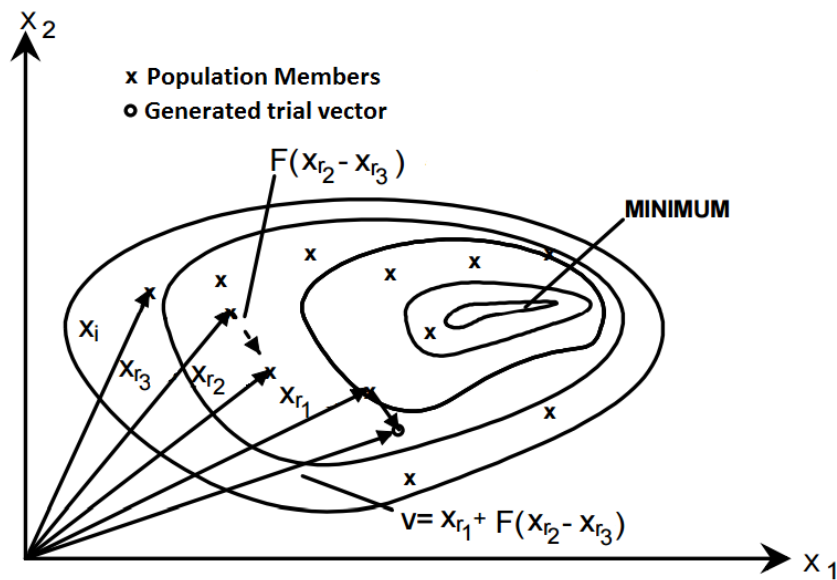


Figure 59: Generation of trial vector for two-dimensional space

After that, crossover operation between obtained trail vector ( $v$ ) and current vector ( $x_i$ ) is performed with a crossover probability of  $c_r$ . Yielding trail member as a result of crossover operation is evaluated for its fitness value. Finally, replacement of current member ( $x_i$ ) with yielding trail member takes place if better fitness value is obtained with yielding trail member.

Structure of the differential evolution algorithm:

---

*Initialize population (  $x_i, i = 1, 2, \dots, NP$ ) randomly*  
*Evaluate fitness of the each population member*  
**do**  $i=1, \text{NumberOfIteration}$   
**do**  $j=1, NP$   
    *select randomly three different members from existing population*  
    ( $x_{r1}, x_{r2}, x_{r3}$ )  
    *generate trail vector:  $v = x_{r1} + \beta \cdot (x_{r2} - x_{r3})$*   
    *perform an crossover operation between trail ( $v$ ) and current vector ( $x_i$ )*  
    *evaluate the fitness of the final trail vector*  
    **if** (*fitness of the trail vector < fitness of the current vector*) **then**  
        *replace the current vector with trail vector*  
    **end if**  
**end do**  
*determine the best member among the population members*  
**end do**

---

### 3.4.4 Genetic Algorithm

The genetic algorithm is a meta-heuristic optimization technique benefiting from the basis of genetics and natural selection. Apart from the most of other optimization algorithms in which population members (solutions) correspond to vector of real numbers, each member of population in genetic algorithm (GA) is represented by a string which is composed of 1s and 0s. In literature, there are many different optimization problems in which genetic algorithm is employed successfully such as pattern recognition, robotics, electronic circuit design and airfoil shape optimization. Although the algorithm can take a special form depending on the type of the problem, main elements remaining common for GA at all of the problems can be stated as chromosomes, selection, crossover and mutation. These elements are explained more explicitly in next paragraph.

In GA, population is constituted by chromosomes which can be thought as candidate solutions for the given problem. Reproduction of the population is essential if existing solutions do not meet requirements. For this purpose, selection process is achieved by considering the calculated fitness values of existing chromosomes, that is, it is likely possible to select chromosomes having better fitness values. Then, crossover operation is implemented on selected chromosome pairs to produce new candidate solutions (new offsprings) with a crossover probability of  $p_c$ . Newly generated offsprings are subjected to mutation with a probability of  $p_m$  (usually very small). Representative figures which demonstrate crossover and mutation operation over chromosome pairs can be seen in Figure 60 and 61:

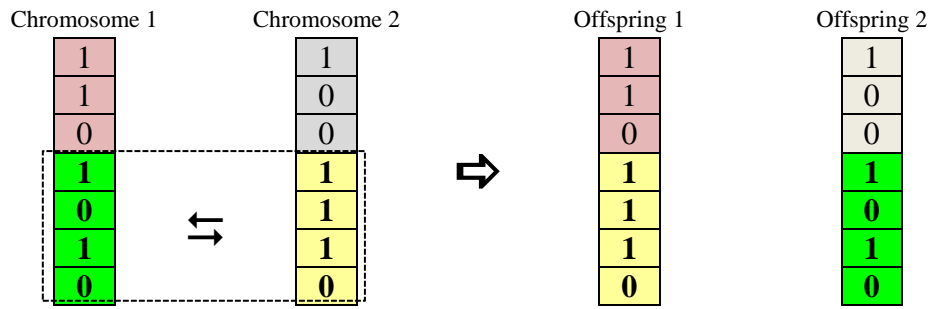


Figure 60: Crossover operation

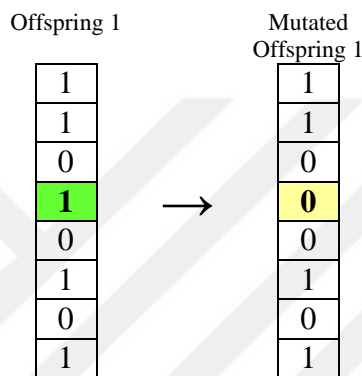


Figure 61: Mutation operation

Structure of genetic algorithm:

---

*Initialize the population randomly with  $n$  chromosomes*

**do**  $j=1, \text{NumberOfGeneration}$

*Calculate the fitness value of the each chromosome in the population*

*Determine the best chromosome*

**do while** (*number of generated offsprings  $\neq n$* )

*Select a pair of chromosomes from the current population*

*Employ crossover operator to the selected pair chromosomes*

*Implement mutation operator to the newly generated offsprings*

*Place new offsprings in the new population*

**end do**

**end do**

---

## CHAPTER 4

### RESULTS AND DISCUSSION

In this section, results of the optimization studies performed throughout this work are presented. The purpose of these optimization studies is to achieve an inverse design of the ramjet missile configuration shown in Figure 16. At the end of the optimization studies, the most appropriate missile configuration, determined by checking agreement with the target missile configuration's (TMC) aerodynamic coefficients and design parameters, is obtained among the evaluated candidate missile configurations (CMC). The CMC refers to Candidate Missile Configurations that are produced and evaluated throughout generations during the optimization process. On the other hand, TMC corresponds to Target Missile Configuration, which has certain performance values and design parameters.

In this study, optimization studies are conducted for two specific cases. In the first case, the purpose is to evaluate success of available optimization algorithms by employing in the inverse design. In this case, aerodynamic coefficients of both CMC and TMC are calculated by means of Missile DATCOM fast prediction tool. In the second case, similar optimization study as such in the previous one is performed. In this case, best optimization algorithm which is determined depending on the competitive results of the first case is selected to be employed. During the design optimization process, aerodynamic coefficients of candidate missile configurations are calculated by improved method and it is made use of experimental data for the target missile configuration. Also, additional optimization study for the second case is performed by using Missile DATCOM analysis tool in place of the improved method. Comparison of optimization studies in the second case will show to what

extent the design optimization process will be enhanced if improved method is used in place of Missile DATCOM analysis tool.

#### 4.1 Design Variables and Objective Function

During the design optimization tasks, design variables play crucial role to calculate value of the objective function. In this chapter, optimization studies are performed depending on the design variables presented below;

$$x = \begin{bmatrix} x_1 \\ x_2 \\ x_3 \\ x_4 \end{bmatrix} = \begin{bmatrix} \text{Span} \\ \text{Chord} \\ \text{Taper Ratio} \\ \text{Leading Edge} \end{bmatrix}$$

Visual representation of the design variables on the missile configuration can be seen in the figure below:

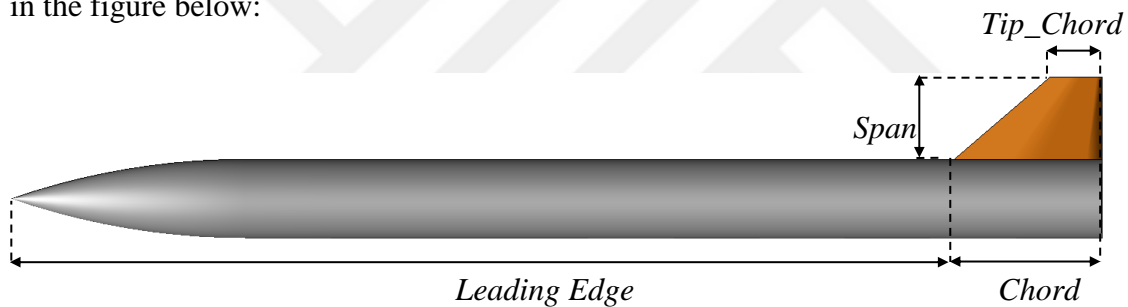


Figure 62: Representation of design variables on missile configuration

$$\text{where; } \text{Taper Ratio} = \frac{\text{Tip\_Chord}}{\text{Chord}}$$

Optimization studies are carried out depending on the design variables which are within the defined constraints. Constraints for the design variables can be seen in Table 8:

Table 8: Lower and upper limits of design variables

Design Variables	Unit	Lower Limit	Upper limit	Target
Span	cm	2.0	20.0	8.05
Chord	cm	5.0	25.0	14.67
Taper Ratio	-	0.0	1.0	0.346
Leading Edge	cm	80.0	100.0	92.00

The objective function consisting of three sub-objective functions ( $F_1$ ,  $F_2$  and  $F_3$ ) is calculated by the corresponding candidate missile configuration aerodynamic coefficients. Each sub-objective function refers to evaluation of static aerodynamic coefficients at particular Mach number. Summation of the normalized differences between target missile configuration (TMC) and candidate missile configuration (CMC) aerodynamic coefficients at corresponding angle of attacks give the sub-objective function value. Details of the objective function can be seen below:

$$\alpha = \begin{bmatrix} 0^\circ \\ 5^\circ \\ 10^\circ \\ 15^\circ \\ 20^\circ \end{bmatrix}, \quad N = 5$$

$$\begin{aligned} \bullet \quad F_1 = \sum_{i=1}^N & \left( \text{abs} \left( \frac{C_{A|TMC} - C_{A|CMC}}{C_{A|TMC}} \right) + \text{abs} \left( \frac{C_{N|TMC} - C_{N|CMC}}{C_{N|TMC}} \right) \right. \\ & \left. + \text{abs} \left( \frac{C_{m|TMC} - C_{m|CMC}}{C_{m|TMC}} \right) \right)_{\alpha=\alpha(i), M=2.5} \end{aligned} \quad (4.1)$$

$$\begin{aligned} \bullet \quad F_2 = \sum_{i=1}^N & \left( \text{abs} \left( \frac{C_{A|TMC} - C_{A|CMC}}{C_{A|TMC}} \right) + \text{abs} \left( \frac{C_{N|TMC} - C_{N|CMC}}{C_{N|TMC}} \right) \right. \\ & \left. + \text{abs} \left( \frac{C_{m|TMC} - C_{m|CMC}}{C_{m|TMC}} \right) \right)_{\alpha=\alpha(i), M=2.95} \end{aligned} \quad (4.2)$$

$$\begin{aligned}
\bullet F_3 = \sum_{i=1}^N & \left( abs \left( \frac{C_{A|TMC} - C_{A|CMC}}{C_{A|TMC}} \right) + abs \left( \frac{C_{N|TMC} - C_{N|CMC}}{C_{N|TMC}} \right) \right. \\
& \left. + abs \left( \frac{C_{m|TMC} - C_{m|CMC}}{C_{m|TMC}} \right) \right)_{\alpha=\alpha(i), M=3.5}
\end{aligned} \tag{4.3}$$

$$\bullet F_{Total} = F_1 + F_2 + F_3 \tag{4.4}$$

Summation of the sub-objective functions gives the total objective function value. During design optimization process, it is aimed to reach a condition in which total objective function value is converged to zero. In this condition, it is expected that the candidate missile configuration design parameters become equivalent to target missile configuration design parameters.

In this study, it is mainly focused on two specific cases (Case 1 and Case 2) for the inverse design optimization. For the optimization studies of these cases, objective function, design variables and their constraints are considered as stated in this section.

#### **4.2 Case 1: Inverse Design Optimization Studies with Fast Prediction Method (Missile DATCOM)**

In this section, inverse design studies are accomplished with available optimization algorithms to determine most suitable algorithm which will be used for optimization studies of the next case. Selection of the algorithm is achieved by the comparative analyses of results of the current inverse design study.

Throughout the optimization studies, Missile DATCOM fast prediction tool is used to calculate candidate missile configuration aerodynamic coefficients. In addition, target missile configuration predetermined aerodynamic coefficients are also calculated by the Missile DATCOM fast prediction tool. In this case, it is highly possible to have a value of objective function converged to zero during analyses

since the candidate configuration aerodynamic coefficients can exactly match the corresponding coefficients of the target configuration.

Before starting the analyses, population size and maximum iteration number for all algorithms are initialized to 100 and 4000, respectively. Then, analyses are performed with stated initialized parameters for three different initial numbers which are 12017, 35871 and 77865. Summary of converged iteration numbers of optimization algorithms and comparative representation of objective function values with respect to iteration number for all algorithms can be seen in Table 9 and Figure 63-66, respectively:

Table 9: Summary of converged iteration numbers of optimization algorithms

Algorithm	IRN=12017	IRN=35871	IRN=77865
MCS	415	802	378
DE	1892	1087	1051
GA	4000	4000	4000

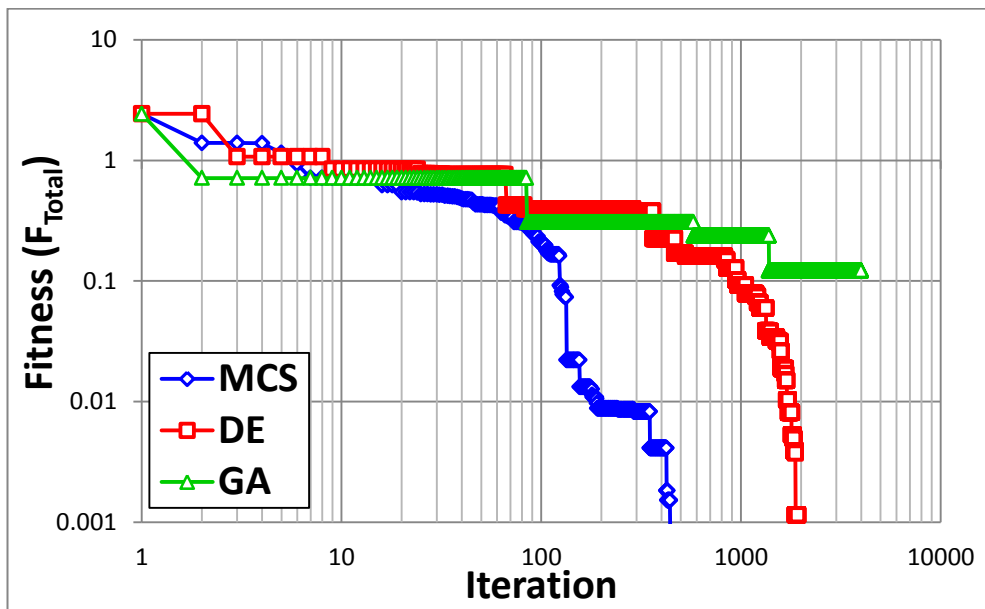


Figure 63: Change of fitness value ( $F_{Total}$ ) with respect to iteration number (IRN=12017)

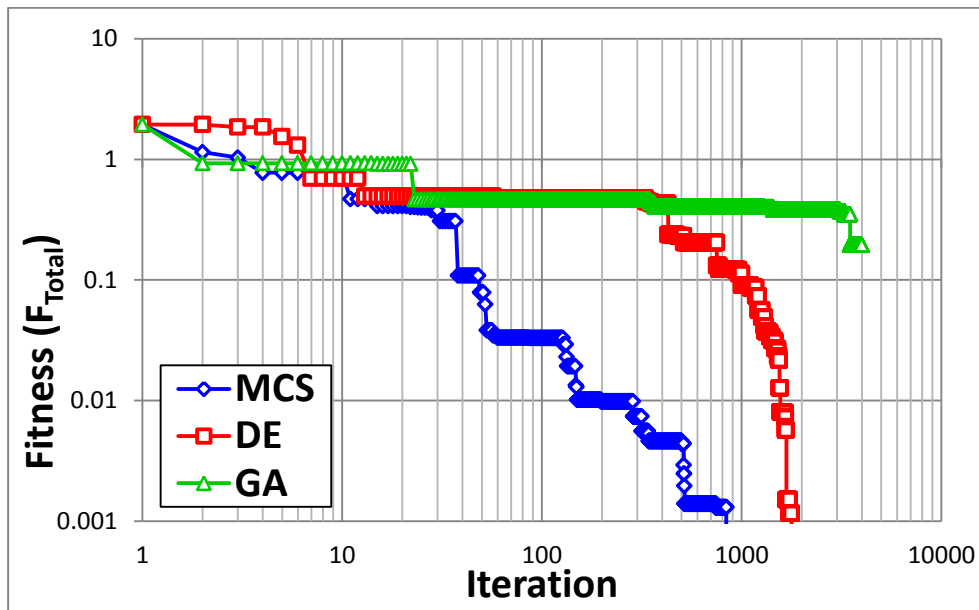


Figure 64: Change of fitness value ( $F_{Total}$ ) with respect to iteration number (IRN=35871)

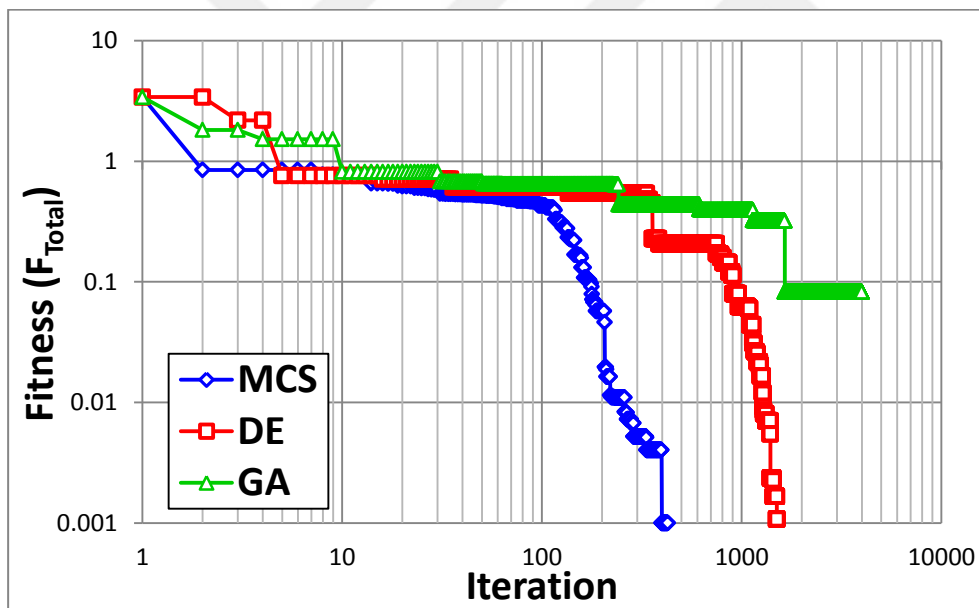


Figure 65: Change of fitness value ( $F_{Total}$ ) with respect to iteration number (IRN=77865)

Visual representation of optimum configurations for corresponding optimization algorithms at selected iteration number can be seen in Figure 66-68:

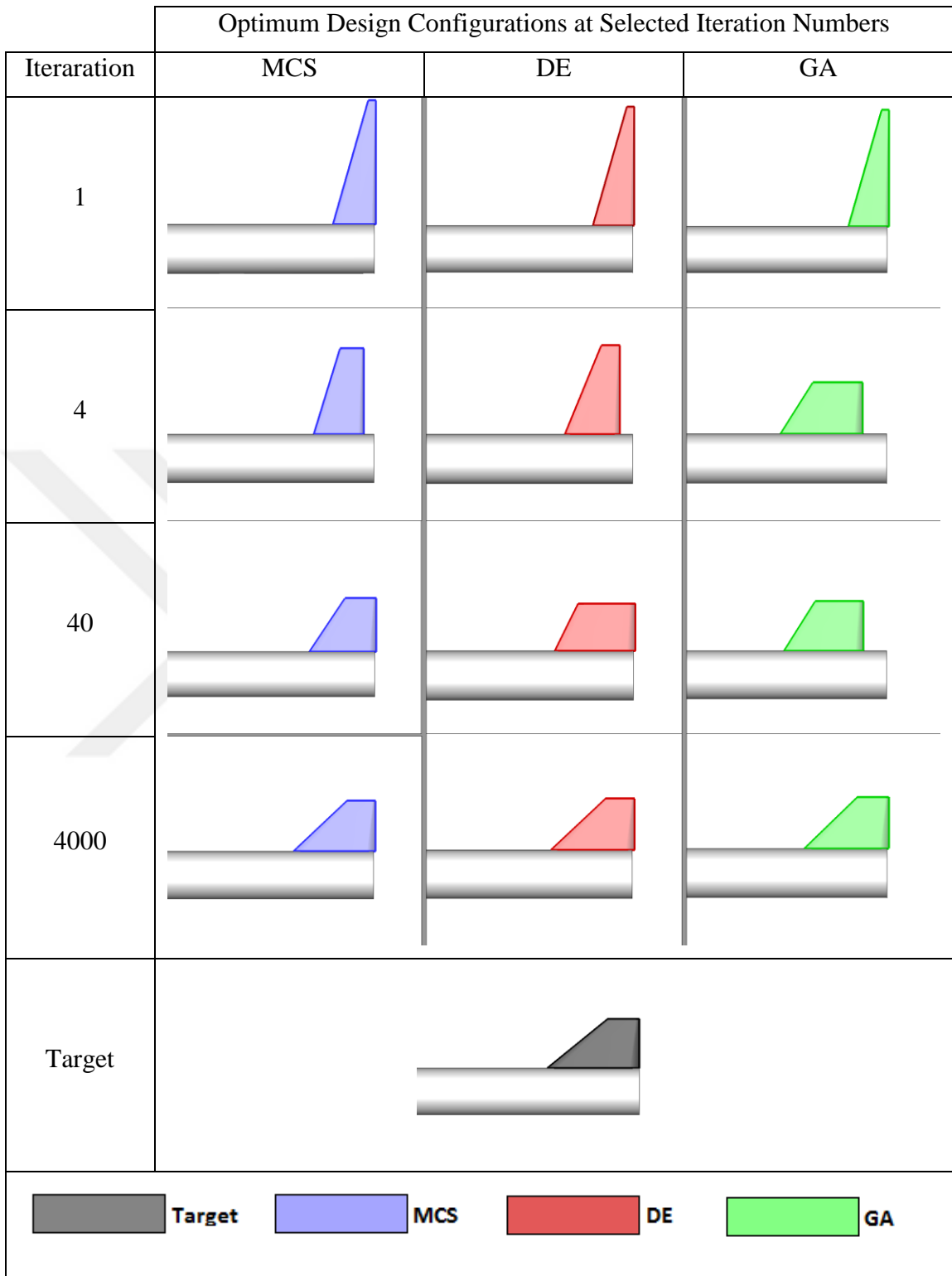


Figure 66: Configuration history of the design optimization studies (IRN=12017)

Optimum Design Configurations at Selected Iteration Numbers			
Iteration	MCS	DE	GA
1			
4			
40			
4000			
Target			

Figure 67: Configuration history of the design optimization studies (IRN=35871)

Optimum Design Configurations at Selected Iteration Numbers			
Iteration	MCS	DE	GA
1			
4			
40			
4000			
Target			

Figure 68: Configuration history of the design optimization studies (IRN=77865)

Available optimization algorithms can be compared in terms of their convergence speed which is directly related to success of obtaining the target missile configuration design variables. As it is seen obviously from Table 9, modified cuckoo search has a better convergence speed for optimization studies driven with three different initial random numbers. As a result, it can be deduced that modified cuckoo algorithm is more suitable than differential evolution and genetic algorithm to be used during the design optimization task of the second case.

### **4.3 Case 2: Inverse Design Optimization Studies with Improved Method**

In this part, details of the design optimization studies, which are carried out by using the optimization algorithm of modified cuckoo search selected after achieving comparative study of first case, are presented. Design variables and their constraints used throughout the optimization process of this case are same as those used for the previous case. This study differs from the previous one with two aspects. Those aspects are respectively the method used for calculating missile configuration aerodynamic coefficients and target missile configuration predetermined aerodynamic coefficient values in the objective function. In the objective function, candidate configuration missile aerodynamic coefficients are calculated by the improved method while target configuration missile predetermined aerodynamic coefficients are gained from the experimental results [4].

In this case, another optimization study in which Missile DATCOM fast prediction tool is used instead of improved method to calculate candidate missile configuration aerodynamic coefficients is also conducted. Results of this study will help to show how preliminary design phase can be improved by using improved method in place of Missile DATCOM fast prediction tool.

Before starting design optimization analyses, initialization of some parameters used in the modified cuckoo search optimization algorithm can be seen in Table 10:

Table 10: Assigned values of the optimization algorithm parameters

Parameters	Value
Population Size	100
# of elite eggs	25
# of non-elite eggs	75
Initial Random Number	14857
Discard Probability	0.7

After accomplishing analyses of the both optimization studies, output of the objective functions and the corresponding design variables are obtained. Change of the objective functions values for each study with respect to iteration number can be seen in Figure 69:

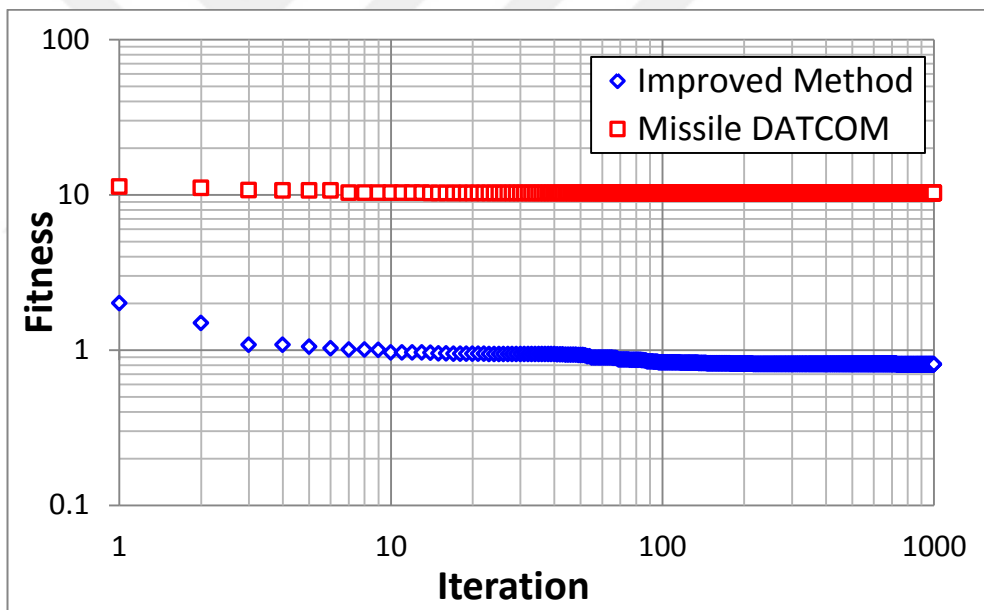


Figure 69: Fitness value variation of the design optimization studies

Since the optimization algorithm used in this case is evolutionary based, many other alternative design configurations are evaluated during the optimization process. To include these alternative design configurations, it is utilized Pareto Frontier [12] which is used to find set of nondominated solutions (potentially optimal solutions) in the solution domain.

In this study, total objective function consists of three sub-objective functions. This characteristic of the total objective function enables the application of pareto frontier method. Comparison of sub-objective function values of the pareto and non-pareto design configurations for improved method are shown in Figure 71, 72 and 73.

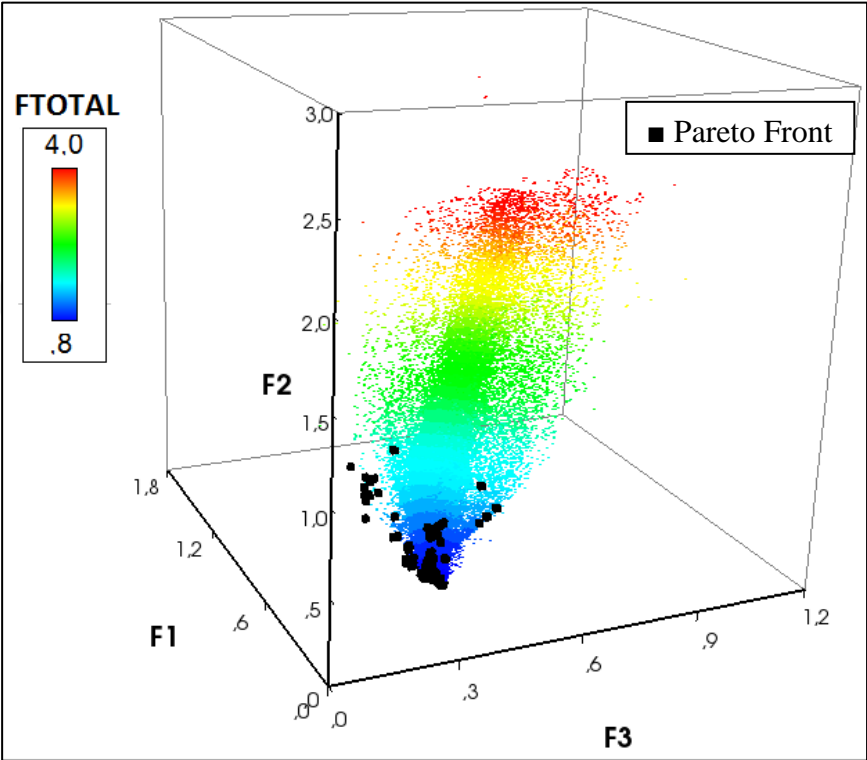


Figure 70: Comparison of the sub-objective functions in 3D

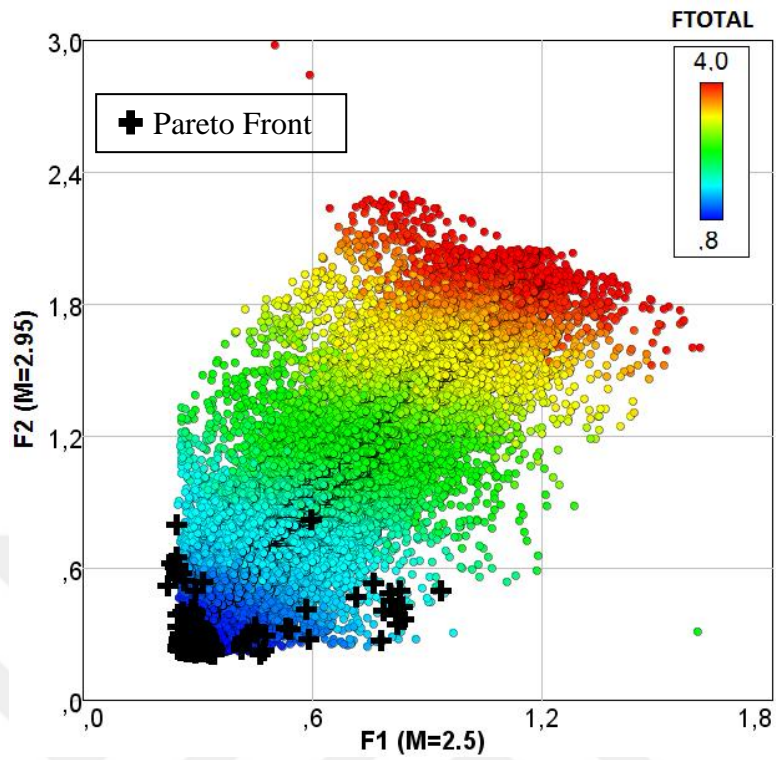


Figure 71: Demonstration of improved method output data with pareto designs

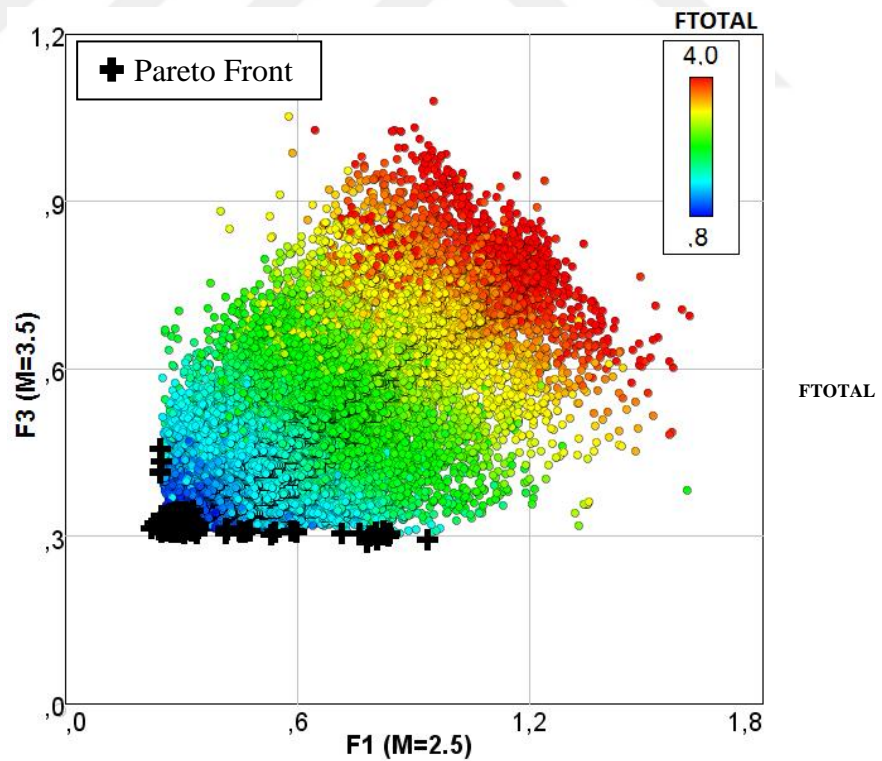


Figure 72: Demonstration of improved method output data with pareto designs

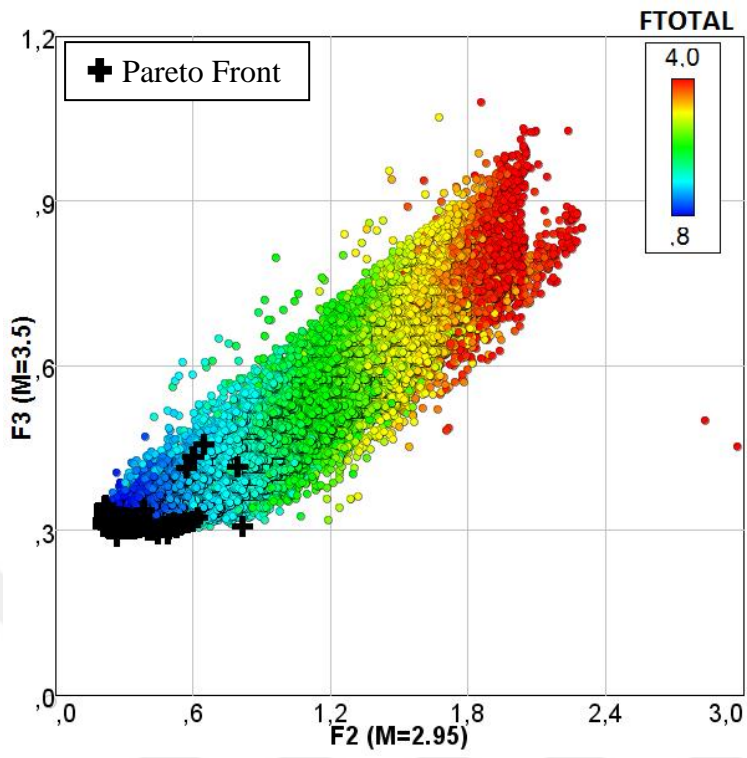


Figure 73: Demonstration of improved method output data with pareto designs

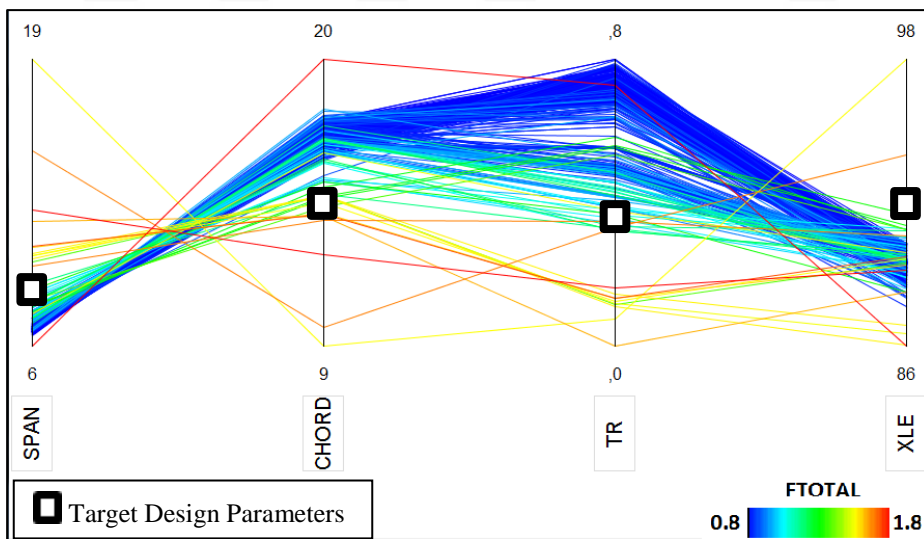


Figure 74: Parallel coordinates plots of improved method pareto designs

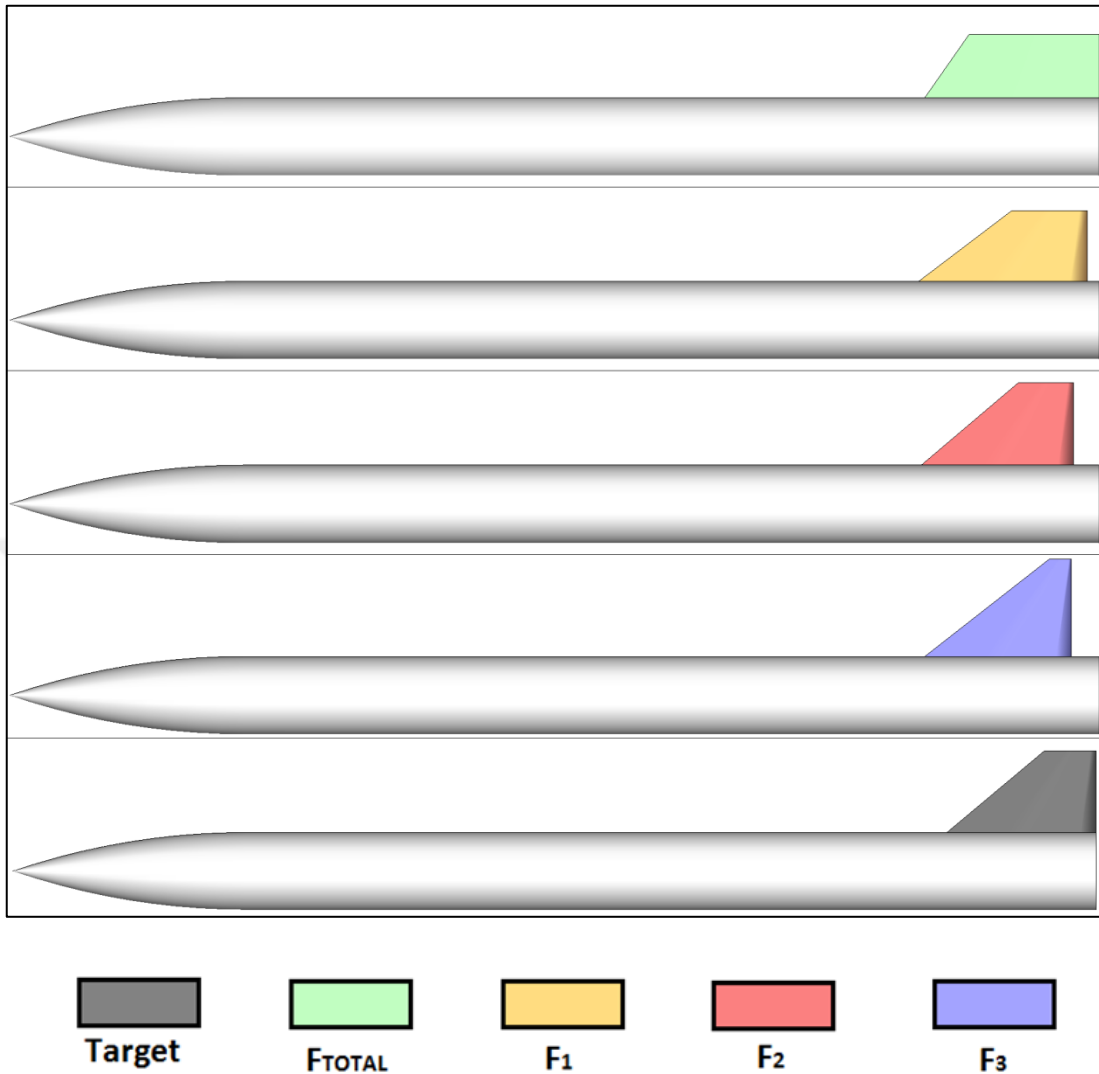


Figure 75: Presentation of improved method pareto design configurations for total objective function and each sub-objective function

- Target** : Target Configuration
- $F_{TOTAL}$**  : Pareto Design Configuration having minimum  $F_{TOTAL}$  value
- $F_1$**  : Pareto Design Configuration having minimum  $F_1$  value
- $F_2$**  : Pareto Design Configuration having minimum  $F_2$  value
- $F_3$**  : Pareto Design Configuration having minimum  $F_3$  value

Pareto analyses are also achieved on the data obtained from the optimization study which is driven with Missile DATCOM instead of the improved method.

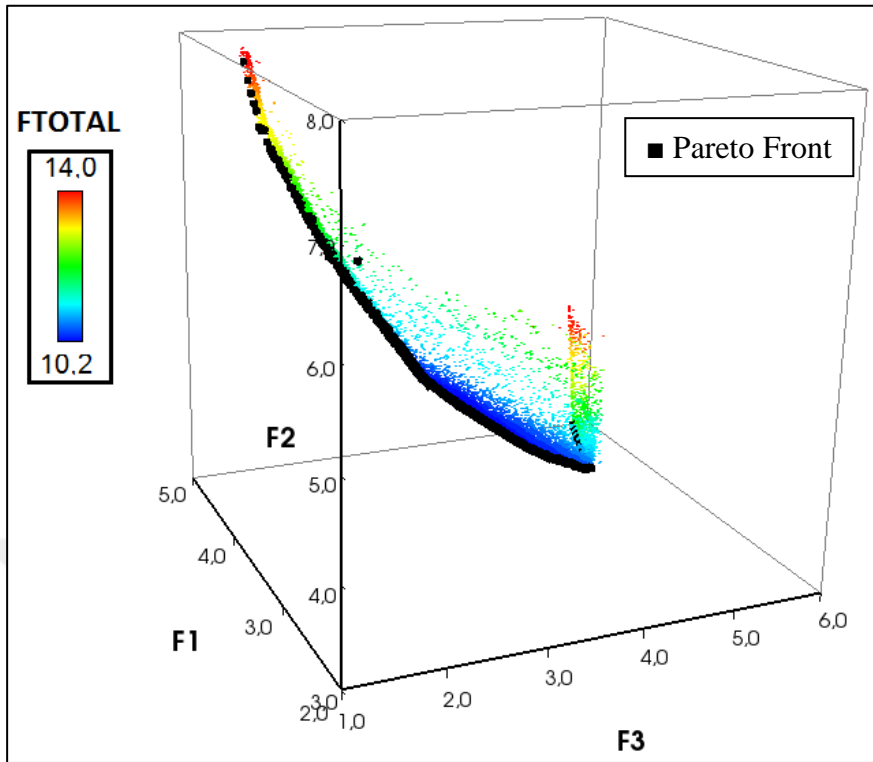


Figure 76: Comparison of the sub-objective functions in 3D

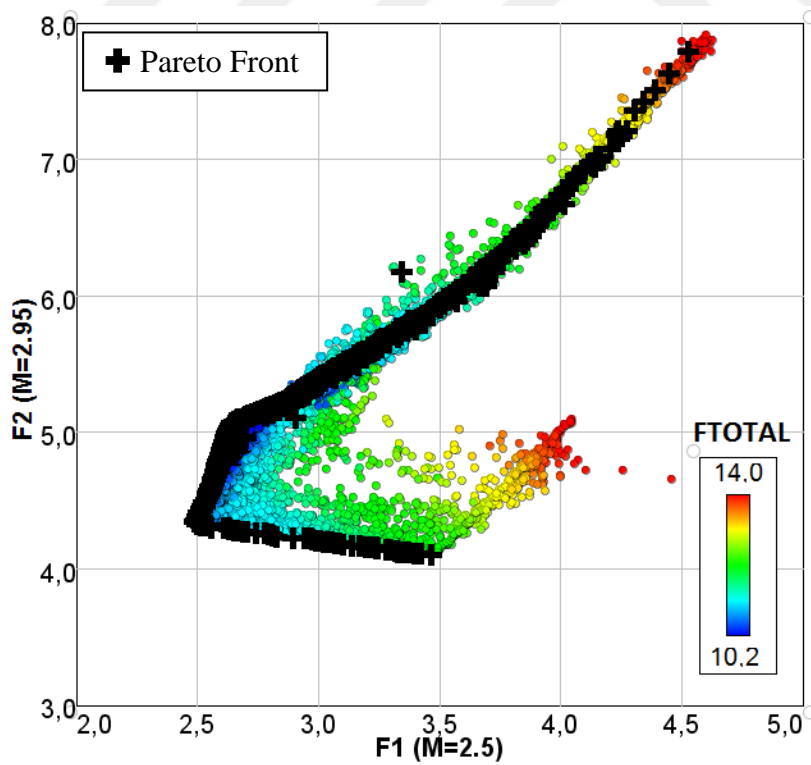


Figure 77: Demonstration of Missile DATCOM output data with pareto designs

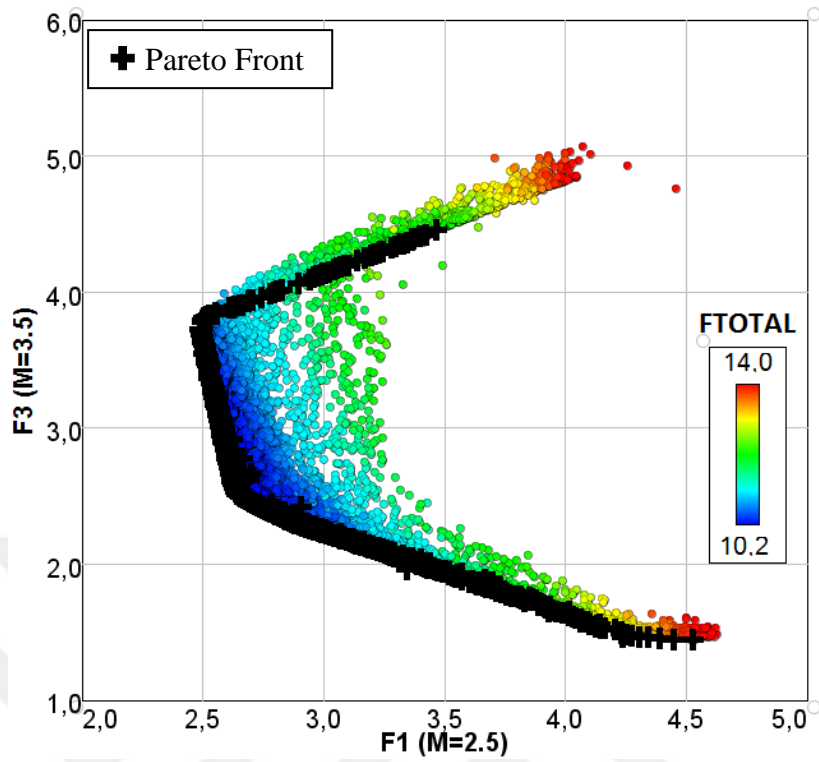


Figure 78: Demonstration of Missile DATCOM output data with pareto designs

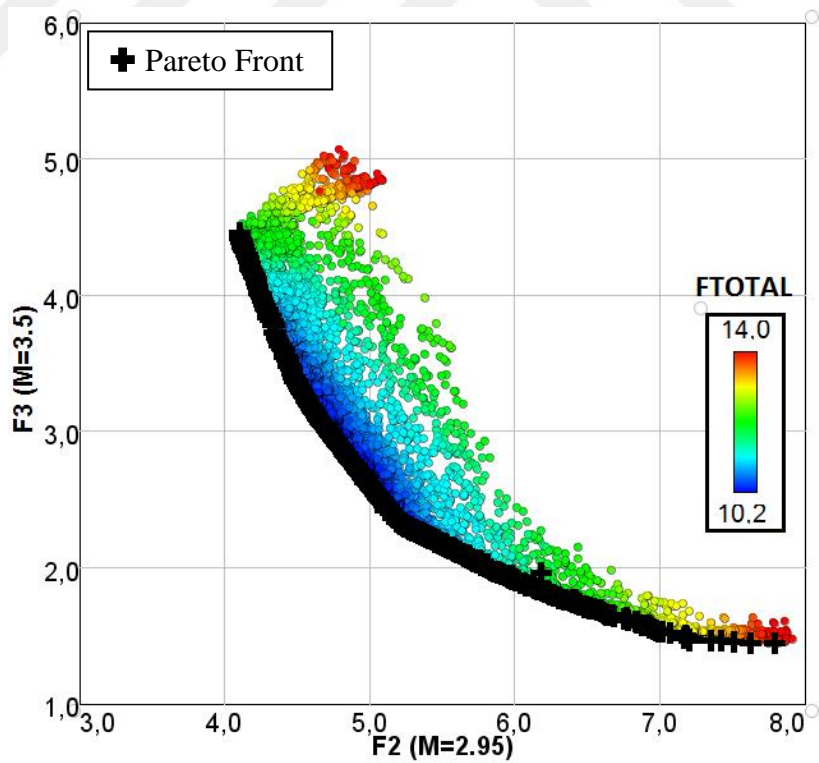


Figure 79: Demonstration of Missile DATCOM output data with pareto designs

Corresponding parallel coordinates plots of this optimization study can be seen in the figure below:

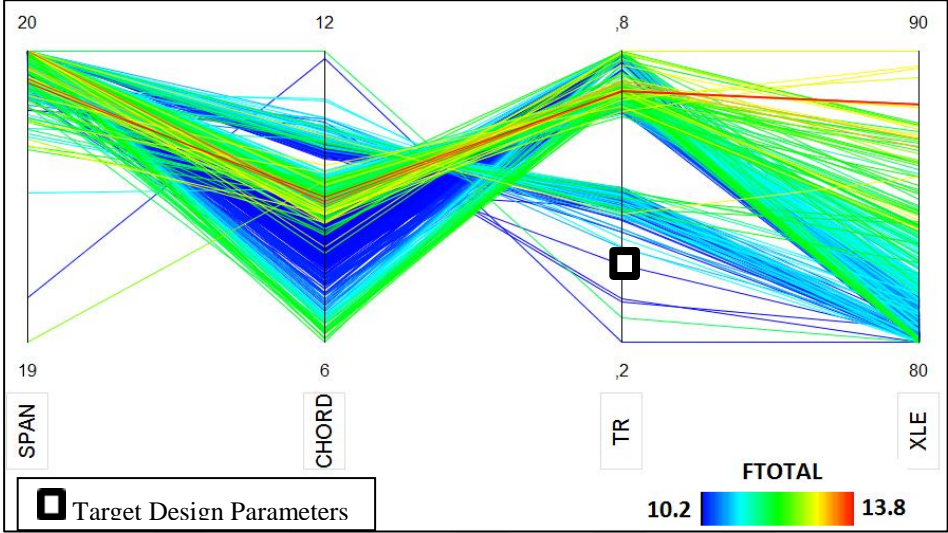


Figure 80: Parallel coordinates plots of Missile DATCOM pareto designs

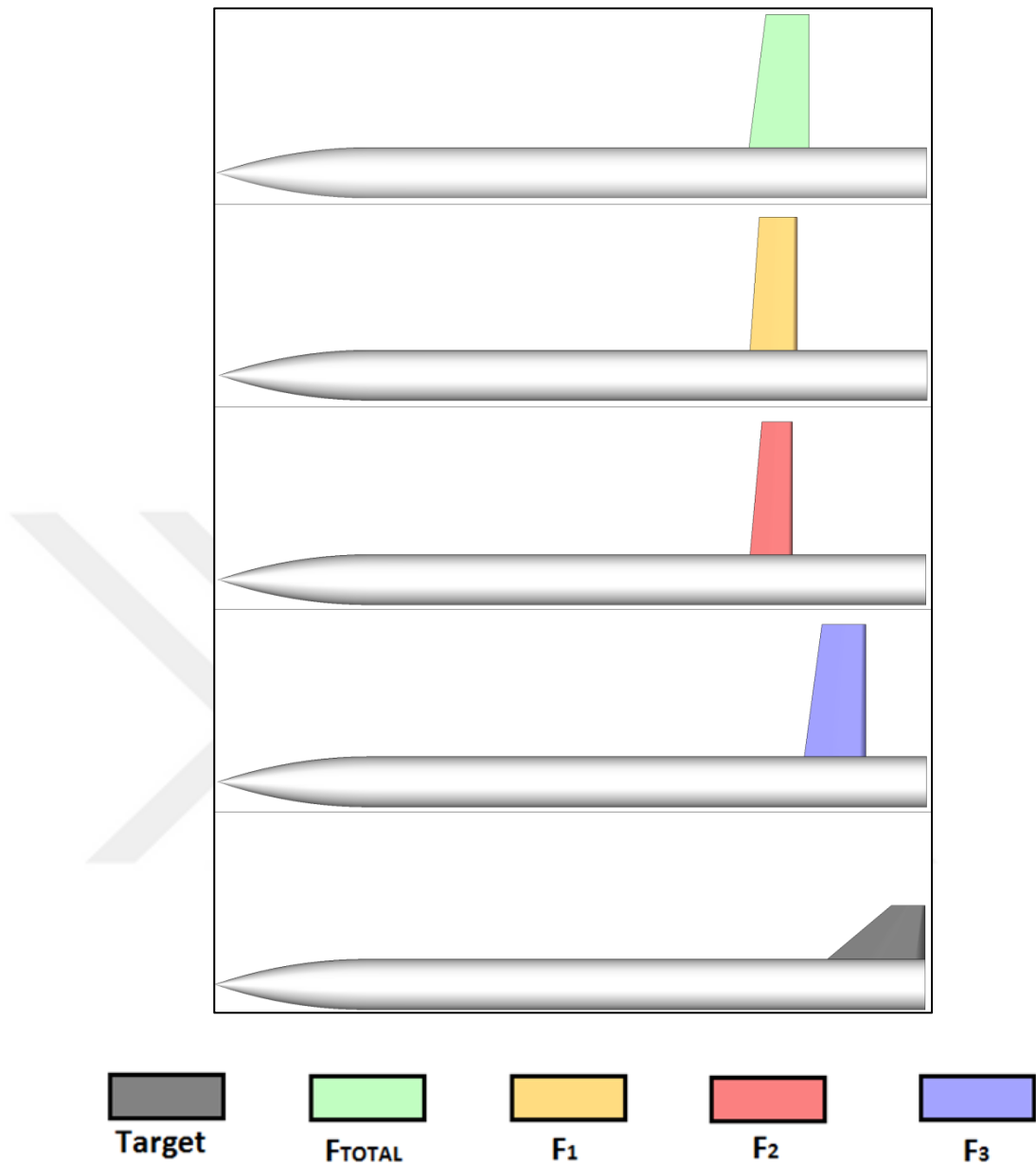


Figure 81: Presentation of Missile DATCOM pareto design configurations for total objective function and each sub-objective function

- Target** : Target Configuration
- F<sub>TOTAL</sub>** : Pareto Design Configuration having minimum F<sub>TOTAL</sub> value
- F<sub>1</sub>** : Pareto Design Configuration having minimum F<sub>1</sub> value
- F<sub>2</sub>** : Pareto Design Configuration having minimum F<sub>2</sub> value
- F<sub>3</sub>** : Pareto Design Configuration having minimum F<sub>3</sub> value

Pareto analyses on the output data of the optimization studies are achieved by means of the Advanced Trade Space Visualization [30] software and pareto design configurations are highlighted with black plus markers (+) in the figures. After extracting pareto design configurations from output data, parallel coordinates graphs of these configurations are plotted and shown in Figure 74 and 80. By comparing the alternative design configurations shown in the parallel coordinate graphs, the improved method can be interpreted as better than Missile DATCOM to produce similar design configurations to the target design configuration.

Output design parameter values of the best pareto design configurations are summarized in Table 11:

Table 11: Comparison of the optimum configurations obtained at the end of the design optimization studies

<b>Parameter</b>	<b>Configuration 1</b> <i>(Improved Method)</i>	<b>Configuration 2</b> <i>(Missile DATCOM)</i>	<b>Target</b>
Span	6.175	19.993	<b>8.05</b>
Chord	17.115	9.035	<b>14.67</b>
Taper Ratio	0.7515	0.7187	<b>0.346</b>
Leading Edge	89.56	80.001	<b>92.0</b>
Fitness	0.8085	10.2208	<b>0.0</b>

In Table 11, the output configurations obtained as a result of design optimization studies carried out by two different methods (Improved Method, Missile Datcom) can be compared in terms of the agreement of the design parameters with the target configuration. From table, it is seen that the missile configurations having design parameter values closer to the target configuration can be reached by applying the improved method instead of Missile DATCOM. Therefore, it can be interpreted that design success during the preliminary design phase can be improved as accuracy of the prediction of aerodynamic coefficients is increased.

In Table 11, it is seen that converged design parameter values obtained at the end of the optimization studies do not exactly match the values of the target configuration design parameters. The reason of this can be explained by examining the Figure 17-25. From the figures, it is seen that calculated aerodynamic coefficients with improved method and Missile DATCOM do not exactly agree with experimental data at corresponding angle of attacks. Therefore, it is not possible both obtaining zero objective function value and target configuration design parameters at the end of design optimization process for this case.





## CHAPTER 5

### CONCLUSION

The purpose of this study was to develop an improved method planned to be used as a tool calculating aerodynamic coefficients of ramjet missiles accurately, and perform inverse design optimizations of ramjet missiles with developed method to achieve enhanced results. In literature, short-term design optimization tasks having usually inaccurate results are carried out by using the fast prediction tools. On the other hand, long-term design optimization tasks having accurate results are carried out by using the CFD tools. This study sought to answer the question whether it is possible to achieve both relatively short-term and relatively accurate results for design optimization tasks.

During the analyses concerning the design optimization task of ramjet missiles, tail fin set geometry of ramjet missiles were within the scope. Designing of the body and ramjet components were out of the scope and their contributions to aerodynamic loads were calculated by means of CFD tools since their geometries were fixed. Contribution of the tail fin set component to aerodynamic loads was provided through fast prediction tool which significantly increased design optimization task speed.

The prediction of aerodynamic coefficients of ramjet missiles throughout this study was succeeded for the geometry having one tail fin set. As number of the tail fin sets on the missile increase, prediction accuracy for aerodynamic coefficients is expected to be decreased.

Design optimization tasks performed throughout this study could also be achieved by the help of the gradient-based optimization algorithms. However, it would be almost impossible to get global optimum point in the design spaces with gradient-based algorithms since there were many local optimum points in the design space in addition to global optimum point. Therefore, it is inevitable of using metaheuristic type optimization algorithms for this kind of design optimization tasks.

Results of this study show that success of the design optimization tasks can be significantly enhanced by using the developed method. By employing the improved method, mistaken performance prediction can be prevented and ideal fin set geometries can be designed.

## REFERENCES

- [1] P. J. Waltrup, F. Zarlingo and E. S. Gravlin, "History of Ramjet and Scramjet Propulsion Development for U.S. Navy Missiles," *JOHNS HOPKINS APL TECHNICAL DIGEST*, vol. 18, 1997.
- [2] "Ramjet," Wikipedia Foundation, [Online]. Available: <https://en.wikipedia.org/wiki/Ramjet>. [Accessed 22 12 2016].
- [3] E. L. Fleeman, *Tactical Missile Design*, AIAA Education Series, 2001.
- [4] H. Clayde, "Aerodynamic Characteristics of a Series of Twin-Inlet Air-Breathing Missile Configurations II - Two-Dimensional Inlets at Supersonic Speeds," NASA, Hampton, Virginia, 1983.
- [5] R. S. Fry, "The U.S. Navy's Contribution to Airbreathing Missile Propulsion Technology," in *AIAA Centennial of Naval Aviation Forum "100 Years of Achievement and Progress"*, Virginia, 2011.
- [6] "Meteor Missile Photo," [Online]. Available: <http://www.defenseindustrydaily.com/meteor-missile-will-make-changes-to-accommodate-f35-0599/>. [Accessed 07 12 2016].
- [7] "Moskit Missile Photo," [Online]. Available: <http://www.ausairpower.net/APA-Rus-Cruise-Missiles.html#mozTocId589963>. [Accessed 03 12 2016].

- [8] "Talos Missile Photos," [Online]. Available: <http://postwarv2.com/talos/photos.html>. [Accessed 2016 12 02].
- [9] R. J. Hartfield, R. M. Jenkins and J. E. Burkhalter, "Ramjet Powered Missile Design Using a Genetic Algorithm," in *42nd AIAA Aerospace Sciences Meeting and Exhibit*, Reno, Nevada, 2004.
- [10] M. B. Anderson, J. E. Burkhalter and R. M. Jenkins, "Missile Aerodynamic Shape Optimization Using Genetic Algorithms," in *AIAA 37th Aerospace Sciences Meeting*, Reno, 1999.
- [11] M. Baratech, J. Ceva, J. Chaklos, J. L. Martinez, J. Winkelmann and D. K. Ravindra, "Preliminary Design of a Ramjet Powered Supersonix Anti-Ship Missile," in *Aircraft Design and Operations Meeting*, Baltimore, 1991.
- [12] A. Gaiddon and D. Knight, "Aerodynamic Optimization of the Aeropropulsive System of a Ramjet Powered Missile," in *9th AIAA/ISSMO Symposium on Multidisciplinary Analysis and Optimization*, Atlanta, 2002.
- [13] J. Moerel, R. F. Calzone, W. Halswijk, R. V. D. Horst, R. Stowe and M. Lauzon, "Performance Simulations of a Rocket and a Ramjet Air-to-Air Missile," in *AIAA Modeling and Simulation Technologies Conference and Exhibit*, Montreal, 2001.
- [14] W. W. Herling, "Prediction of the Steady Three-Dimensional Aerodynamics of a Supersonic Ramjet Missile," in *AIAA/SAE/ASME/ASEE 21st Joint Propulsion Conference*, Monterey, 1985.
- [15] R. J. Krieger, "Supersonic Missile Aerodynamic and Performance Relationships for Low Observables Mission Profiles," in *AIAA 9th Atmospheric Flight Mechanics Conference*, San Diego, 1982.

- [16] J. G. Metts, R. J. Hartfield, J. E. Burkhalter and R. M. Jenkins, "Reverse Engineering of Solid Rocket Missiles with a Genetic Algorithm," in *45TH AIAA Aerospace Sciences Meeting and Exhibit*, Reno, Nevada, 2007.
- [17] K. Arslan, "Aerodynamic Optimization of Missile External Configurations," Thesis for the degree of Master of Sciences, Middle East Technical University, ANKARA, 2014.
- [18] D. B. Riddle, R. J. Hartfield, J. E. Burkhalter and R. . M. Jenkins, "Genetic Algorithm Optimization of Liquid Propellant Missile Systems," in *45th AIAA Aerospace Sciences Meeting and Exhibit*, Reno, Nevada, 2007.
- [19] M. Carpenter, R. Hartfield and J. Burkhalter, "A Comprehensive Approach to Cataloging Missile Aeodynamic Performance Using Surrogate Modeling Techniques and Statistical Learning," in *Applied Aerodynamics Conference*, Honolulu, Hawaii, 2011.
- [20] A. E. Çetiner, "Split Canard Design for Enhancing the Maneuverabilityof a Missile at High Angle of Attack," Thesis for the degree of Master of Sciences, Middle East Technical University, ANKARA, 2012.
- [21] X.-S. Yang and S. Deb, "Cuckoo Search via Levy Flight," in *World Congress on Nature & Biologically Inspired Computing*, 2009.
- [22] S. P. Walton, "Gradient Free Optimization in Selected Engineering Applications," Thesis for the degree of Doctor of Philosophy, Swansea University, Swansea, 2013.
- [23] "Beale Function," Wikimedia Foundation, [Online]. Available: [https://en.wikipedia.org/wiki/File:Beale%27s\\_function.pdf](https://en.wikipedia.org/wiki/File:Beale%27s_function.pdf). [Accessed 12 5 2016].

- [24] M. V. G., "Levy flights and superdiffusion in the context of biological encounters and random searches," *Physics of Life Reviews*, 2008.
- [25] W. C. Pitts, J. N. Nielsen and G. E. Kaattari, "Lift and Center of Pressure of Wing-Body-Tail Combinations at Subsonic, Transonic, and Supersonic Speeds," N.A.C.A. Report 1307, 1953.
- [26] A. Bakker, "Applied Computational Fluid Dynamics, Lecture 10 - Turbulence Modelling," 2006.
- [27] O. Reynolds, "On the Dynamical Theory of Incompressible Viscous Fluids and Determination of the Criterion," *Philosophical Transaction of the Royal Society of London*, vol. 186, pp. 123-164, 1895.
- [28] T. H. Shih, W. W. Liou, A. Shabbir, Z. Yang and J. Zhu, "A New k-Epsilon Eddy Viscosity Model for High Reynolds Number Turbulent Flows-Model Development and Validation," in *NASA Technical Memorandum*, Cleveland, 1994.
- [29] P. L. Davis, A. T. Rinehimer and M. Uddin, "A Comparison of RANS-Based Turbulence Modeling for Flow over a Wall-Mounted Square Cylinder," [Online]. Available: [http://www.cd-adapco.com/sites/default/files/technical\\_document/pdf/PRU\\_2012.pdf](http://www.cd-adapco.com/sites/default/files/technical_document/pdf/PRU_2012.pdf). [Accessed 5 6 2016].
- [30] M. Yukish, T. Simpson, D. Spencer, G. Stump, S. Miller, S. Lego and J. O'Hara, "Trade Space Exploration," Pennsylvania State University, 2010. [Online]. Available: <http://www.atsv.psu.edu/>. [Accessed 12 12 2016].
- [31] A. Akgül, H. Y. Akargün, B. Atak, A. E. Çetiner and O. Göker, "Aerodynamic Predictions For NASA Dual Control Missile And Comparison With Experiment," in *OTEH 2011 On Defensive Technologies*, Belgrad, 2011.

- [32] A. Bakker, "Turbulence Models," 2002.
- [33] S. S. Rao, *Engineering Optimization Theory and Practice*, John Wiley & Sons, Inc., 1996.
- [34] C. Rosema, J. Doyle, L. Auman and M. Underwood, "Missile DATCOM User Manual," U.S. Army Aviation & Missile Research, Development and Engineering Center, 2009.
- [35] P. L. Davis, A. T. Rinehimer and M. Uddin, "A Comparison of RANS-Based Turbulence Modeling for Flow over a Wall-Mounted Square Cylinder," in *The CFD Society of Canada*, Canmore, 2012.
- [36] S. Walton, O. Hassan and M. R. Brown, "Modified cuckoo search: A new gradient free optimisation algorithm," *Chaos, Solitons & Fractals*, vol. 44, no. 9, pp. 710-718, 2011.